Section I: Fundamentals of Nanofluids

CHAPTER 1

Synthesis of Nanoparticles and Nanofluids

A. ANGAYARKANNI[a] AND J. PHILIP*[b]

[a] Department of Physics and Nanotechnology, SRMIST, Kattankulathur – 603203, India; [b] SMART Materials Section, Metallurgy and Materials Group, Indira Gandhi Centre for Atomic Research, Kalpakkam – 603102, India
*Email: philip@igcar.gov.in

1.1 Introduction

The term ''nano'' originates from the Greek word ''nanos'', which means ''dwarf''. When the size of a material is on the nanoscale (1–100 nanometers), in at least one of its dimensions, it is referred to as a nanomaterial.[1] Examples of materials with one, two and three dimensions on the nanoscale are layers, nanowires and particles, respectively.[2] The unique properties of nanomaterials have been exploited for a wide range of applications. The need for efficient cooling materials has led to the emergence of a new field of research on nanofluids.[3–34] Several types of nanofluids have been investigated due to their thermal properties, which include suspensions of spherical,[32,35] rod-shaped, nanowire, nanotube,[36,37] and magnetic nanoparticles.[3,9,38] The heat transport in nanofluids has been studied by many researchers to understand the mechanisms involved.[27,39] Moreover, there have been a number of reviews on this topic.[40,41] Conventional heat transfer fluids have very low thermal conductivity compared to solids such as silver, copper, aluminum, and diamond. Thermal energy is sufficient to keep nanoparticles suspended under Brownian motion in base fluids,[42] which is

Soft Matter Series No. 16
Fundamentals and Transport Properties of Nanofluids
Edited by S. M. Sohel Murshed

Published by the Royal Society of Chemistry, www.rsc.org

one of the attractions of using nanofluids for heat transfer applications. The properties that make nanofluids a promising coolant are good thermal conductivity and heat transfer, good stability and good critical heat flux.[43] Studies have shown that relatively small amounts of nanoparticles can enhance the thermal conductivity of base fluids significantly. Different types of nanofluids have been used in a broad range of engineering applications, such as in automobiles, as coolants,[44] in brake fluids,[45] in domestic refrigerators,[46] in solar devices,[47,48] cosmetics, drug delivery,[49] defect sensors,[50] optical filters,[51] hyperthermia,[52] and sealants.[53] Lately, magnetic nanofluids containing superparamagnetic nanoparticles have been shown to exhibit interesting properties that have been exploited in heat transfer,[54,55] sensors[56–60] and magnetic hyperthermia,[61,62] and dye removal,[63,64] among other applications.

1.2 Preparation of Nanoparticles

Nanoparticles can be prepared either *via* top-down or bottom-up approaches.[65] The top-down approach includes methods such as ball milling, etching, laser ablation and electro explosion. The bottom-up approach includes methods such as precipitation techniques, solvothermal processes, hydrothermal processes, and microwave-assisted synthesis. Schematic representations of the synthesis of nanoparticles *via* top-down and bottom-up approaches are shown in Figure 1.1.

1.2.1 Top-down Approach

In the top-down approach, micron-sized particles are reduced to nano-sized particles using different techniques. The reduction of micron-sized colloidal particles *via* mechanical milling in the presence of a liquid carrier and dispersing agent is referred to as the size reduction method. The influencing parameters for this method are plasticity, hardness, composition of the chemical reagents, presence of micro-cracks and defects in a crystalline structure. Particles synthesized *via* this methods are more stable because metal nanoparticles are directly synthesized from their respective metals. Some of the popular techniques used for the preparation of nanoparticles *via* the top-down approach are discussed below.

1.2.1.1 Mechanical Milling

Mechanical milling is the most widely used method for generating materials on the nanoscale. It is used to generate blends and also to manufacture nanocomposites. This method involves the reduction of micron-sized colloidal particles *via* mechanical milling in the presence of a liquid carrier and dispersing agent. The most commonly used method in mechanical milling is the ball milling method, which involves the grinding of a powdered material into extremely fine nanoparticles of 2–20 nm in size. The ball milling

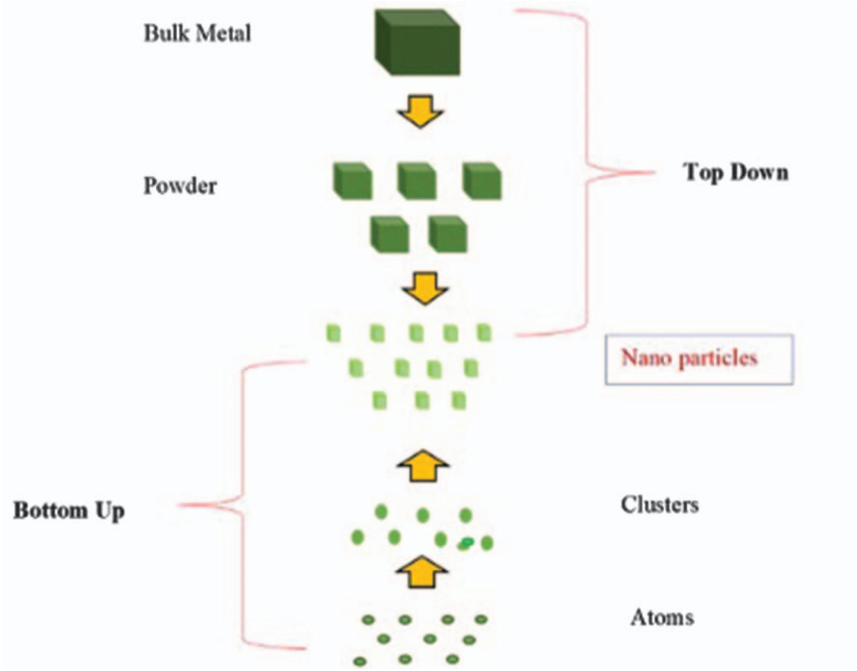

Figure 1.1 Schematic representations of the synthesis of nanoparticles *via* top-down and bottom-up approaches.

chamber consists of a stainless-steel container and many small balls of iron, silicon carbides or tungsten carbides. The balls are allowed to rotate inside the mill along with the material to obtain fine nanoparticles.[66] Carvalho *et al.*[67] synthesized magnetite nanoparticles *via* high energy ball milling using iron powder at a ball-to-powder mass ratio of 20 : 1. Salah *et al.*[68] prepared zinc oxide nanoparticles *via* a ball milling method from its microcrystalline powder in a mixing ratio of 15 : 1 by weight percentage of steel balls and ZnO powder. Alaa El Din Mahmoud *et al.*[69] demonstrated the sustainable synthesis of graphite oxide using a dry ball milling technique employing graphite flakes. A schematic representation of the principles of mechanical (ball) milling is shown in Figure 1.2.

1.2.1.2 Etching

Etching is the process of removing a layer from the surface of a material *via* a chemical reaction in the presence of a strong acid, base or suitable gas. Li *et al.*[70] synthesized concave polyhedral platinum nanoparticles using this method, wherein HCl was used for etching the surface of the platinum nanoparticles. Cheng *et al.*[71] synthesized a Fe–Si binary oxide composite using an organic template, where the Si units were then etched using NaOH to leave iron oxide nanoparticles to adsorb arsenic from water.

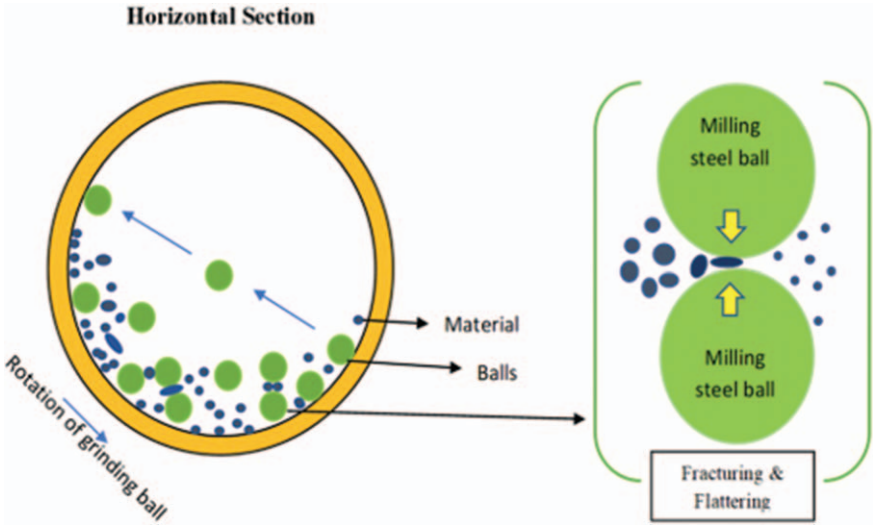

Figure 1.2 Schematic representation of the principles of mechanical ball milling.

1.2.1.3 Laser Ablation

Laser ablation involves the irradiation of a target material with a laser beam, which leads to its vaporization and the formation of nanoparticles. The rate of deposition is dependent on the penetration of the incident laser pulse on the surface of the target material within the penetration depth. Pulsed laser ablation of a liquid is an interesting way to manufacture a colloidal solution of uniform-sized nanoparticles without the further addition of surfactants or ligands. Duque *et al.*[72] used this method to prepare colloidal metal oxide nanoparticles in a liquid environment. The method is also used as a replacement for traditional chemical reduction methods for the synthesis of noble metal nanoparticles. This technique does not require any additional chemicals for the stability of the nanoparticles, hence, the synthesis of stable noble metal nanoparticles using pulsed laser ablation is referred to as a green technique.[73] Ismail *et al.*[74] prepared iron oxide nanoparticles *via* pulsed laser ablation using iron in dimethylformamide and sodium dodecyl sulphate solutions as a target.

1.2.1.4 Electro Explosion

Electro explosion involves the synthesis of nanoparticles *via* the electrical explosion of metal wire. In this method, nanoparticles are synthesized *via* the explosion of a metal wire when a high-density current pulse is passed through it. This method has many advantages over all other methods due to its high energy efficiency, variation in characteristics according to the process parameters, small variation in the size of the synthesized nanoparticles,

stability of the nanoparticles under normal conditions, and high probability to obtain metals, alloys, and oxides and nitrides of metal nanoparticles. Sen *et al.*[75] synthesized Cu, Ag, Fe and Al nanoparticles from their conducting parent materials using an electro explosion of a wire method. Berasategi *et al.*[76] synthesized magnetic nanoparticles *via* the electric explosion of a wire.

1.2.2 Bottom-up Approach

The bottom-up approach includes methods such as electrodeposition, vapor condensation, thermal decomposition, laser pyrolysis, co-precipitation, mechanochemical, sol–gel, solvothermal, hydrothermal, bacterial, and reverse micelle techniques. Some of the popular techniques used for the preparation of nanoparticles *via* a bottom-up approach are discussed below.

1.2.2.1 Precipitation Techniques

Precipitation reactions consist of a nucleation step, followed by particle growth.[77] The simultaneous occurrence of the nucleation and growth processes dictates the particle size and morphology. Due to difficulties in isolating nucleation and growth processes for independent study, the fundamental mechanism of precipitation reactions is still not understood fully. When multiple elements are involved in precipitation (co-precipitation), the process becomes all the more complex. The synthesis of ferrite nanoparticles was carried out by precipitating iron salts in alkaline medium. The advantage of co-precipitation process is that it does not produce or use any toxic intermediates or solvents, and does not require precursor complexes and high temperatures. It has become a popular technique due to its ability to be scaled up, its reproducibility and its eco-friendly reaction conditions.[78]

1.2.2.2 Solvothermal

Solvothermal synthesis is usually performed in autoclaves or reactors by maintaining a pressure of >2000 psi at a temperature of ~200 °C. There are two types of solvothermal processes conducted for the synthesis of ferrite nanoparticles; the solvolysis of metal salt solution and oxidation or neutralization of a mixed metal hydroxide.[79] A typical experimental set up of the solvothermal method is shown in Figure 1.3. In this method, metal oxide nanoparticles are prepared by decomposing organometallic compounds such as metal acetylacetonates in high boiling organic solvents containing surfactants. Fe_3O_4 nanoparticles are prepared by decomposing salts such as $[Fe(acac)_3]$ in the presence of 1,2-hexadecanediol, oleylamine and oleic acid in phenol ether.[80,81] Factors such as the ratios of the starting reagents, such

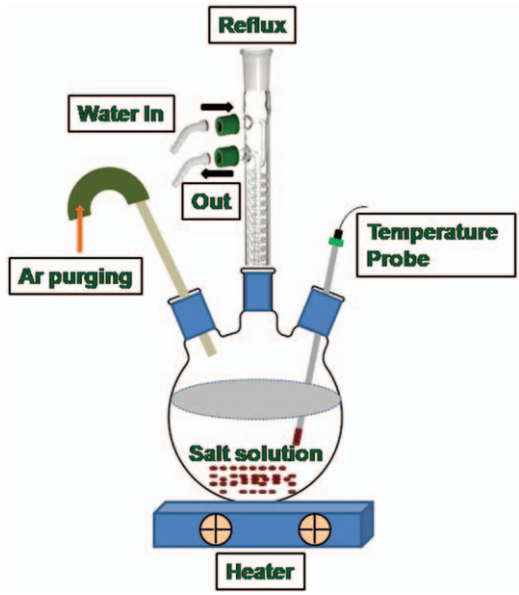

Figure 1.3 Schematic representation of solvothermal synthesis.

as organometallic compounds, surfactant and solvent, are the decisive parameters that control the size and morphology of magnetic nanoparticles. Also, the nature of particles formed in this method depends on the reaction conditions, such as temperature and time.[82]

In this method, the particle size is controlled through a nucleation and growth process. At high reaction temperature, the nucleation might be faster than the growth, while over a long reaction time, the growth process is favored. This method is suitable only for small scale but not for industrial applications due to the high-temperature requirements. Fe_3O_4 nanoparticles prepared in this way are usually dispersed in organic solvent. Recently, it was demonstrated that water soluble Fe_3O_4 nanoparticles (4–60 nm) can be prepared by decomposing $FeCl_3{\cdot}6H_2O$ at 245 °C in the presence of 2-pyrrolidone or α,ω-dicarboxyl-terminated poly(ethylene glycol) as coordinating agents under reflux.[83,84]

1.2.2.3 Flow Injection Method

This method was developed by Alvarez *et al.*[85] and involves the continuous or segmented mixing of precursors under a laminar flow regime in a capillary reactor. The experimental set up includes a multi-channel peristaltic pump, Teflon tubing lines, a T-shaped injector and an injection valve. The advantages of this method are high reproducibility due to plug flow and laminar conditions, a high mixing homogeneity and the precise external control of the process.

1.2.2.4 Decomposition of Metal Carbonyls

This technique is based on the formation of ferromagnetic nanoparticles *via* the thermal decomposition of metal carbonyls in various liquid organic media, gases or under vacuum. At higher temperatures, metal carbonyls decompose and yield metal particles in of the micron-sized range. However, it has been found that in the presence of polymers, these carbonyls decompose into nanosized particles and that it is feasible to change the particle size by selecting the molecular mass and composition (polar and non-polar groups) of the polymer.

1.2.2.5 Reverse Micelle Method

In this method, reverse micelles formed from nanometer-sized droplets of an aqueous phase are stabilized by surfactants in an organic phase and used for the synthesis of nanoparticles.[86] In this technique, surfactant-stabilized water in-oil-emulsions containing the aqueous solution of the precursor are prepared.[87] By mixing two identical water-in-oil micro-emulsions containing the desired reactants, the microdroplets continuously collide, coalesce and finally form a precipitate in the micelles. The precipitate can then be extracted using solvents such as acetone and ethanol by centrifuging the mixture. In this sense, a microemulsion can be used as a nanoreactor for the formation of nanoparticles. Although this method has been used for the synthesis of a wide variety of nanoparticles, the shape and size usually vary over a wide range. The working window is very narrow and only a small amount of material can be prepared using this technique. Moreover, the methods also requires the use of a large amount of solvent.

1.2.2.6 Electrodeposition Technique

This technique was developed on the basis of known practical experience on the subject of preparing metals by electrolysis. The metals are deposited on the cathode as a dense continuous layer, distinctly delimiting single crystals and finely dispersed powders.[88] Using this method, ferromagnetic metals and their alloy-based ferrofluids can be synthesized.[89] The influencing factors of this technique are the cathode surface area, current density, composition of the electrolyte, presence of surfactants and/or additives (such as thiourea, urea, tartaric acid, *etc.*), temperature and agitation of the electrolyte. Electrolysis is performed in a two-layered tank using a needle-shaped cathode sealed in a glass tube, which is lowered and raised periodically. In the two-layered tank, the top layer contains an organic medium, which also contains an appropriate surfactant, and the bottom layer is an aqueous electrolyte solution. After the deposition of nanoparticles at the moving cathode, the metallic nanoparticles are collected in the top non-polar solvent layer containing the surfactant.

1.2.2.7 Sol–Gel Process

Generally, a sol–gel process refers to the hydrolysis and condensation of alkoxide-based precursors. This process contains distinct steps, *i.e.*, (a) the formation of stable solutions of alkoxide or solvated metal precursor, (b) gelation resulting from the formation of an oxide- or alcohol-bridged network *via* a polycondensation or polyesterification reaction, (c) ageing of the gel until the gel transforms into a solid mass, accompanied by concentration of the gel network and expulsion of solvent from the gel pores, (d) drying of the gel, (e) dehydration and (f) decomposition of the gel at high temperature.[90,91] Long *et al.*[92] prepared iron oxide nanoparticles using an iron oxide aerogel obtained from $FeCl_3$ in anhydrous ethanol and epichlorohydrin at a 1 : 10 ratio as a precursor. The dried iron oxide aerogel was decomposed *via* heat treatment at ~300 °C for 20 h. Nanosized iron oxide (ε-Fe_2O_3) with a giant coercivity field (2 T) was prepared by combining micro-emulsion and sol–gel processes.[93]

1.2.2.8 Mechanochemical Reactions

In mechanochemical synthesis, chemical reactions occur at the interfaces of the nanometer-sized grains that are continuously re-generated during milling.[94] Mechanochemical processes that make use of chemical reactions activated by high-energy ball milling have been successfully used for preparing ferrite nanoparticles. Ding *et al.* synthesized $BaFe_{12}O_{19}$ *via* the mechanical milling of a $BaCl_2$, $FeCl_3$ and NaOH powder mixture.[95] Later, other ferrites were prepared *via* the same process using a stoichiometric mixture of an MO (M = Fe, Ni, Zn) and α-Fe_2O_3 as the precursor material.[96–98] Druska *et al.*[96] prepared inverse spinel $ZnFe_2O_4$, instead of normal spinel $ZnFe_2O_4$ *via* the high-energy ball milling of a stoichiometric mixture of ZnO and α-Fe_2O_3.

1.2.2.9 Hydrothermal Synthesis

Hydrothermal synthesis exploits the solubility of almost all inorganic substances in water at elevated temperatures and pressures and results in the subsequent crystallization of the dissolved material from liquid.[90,91] At elevated temperatures, water exists exhibits a high vapor pressure and reactant properties such as solubility and change in reactivity. These changes provide more parameters to tune nucleated particles with different sizes and shapes, which is not possible during low-temperature reactions. The influencing parameters of the process are reaction temperature, pressure, reaction time and salt composition. Recently, Wang *et al.*[99] prepared single-crystalline magnetite nanowires by applying an external magnetic field during the ageing process. It was found that with increasing field, the wire concentration also increases. Zhang *et al.*[100] reported that $NiFe_2O_4$ crystallization in the presence of polyethylene glycol (PEG) produces nanorods.

1.2.2.10 Solvothermal Synthesis

The solvothermal synthesis process is similar to the hydrothermal method but uses solvents other than water. Sun *et al.*[80] reported an organic phase process for synthesizing monodisperse Fe_3O_4 nanoparticles *via* the reaction of $Fe(acac)_3$ and a long-chain alcohol. This reaction was extended to synthesize MFe_2O_4 nanoparticles (M = Co, Ni, Mn, *etc.*) with a tunable size of 3–20 nm in diameter by adding a different metal acetylacetonate precursor to a mixture of $Fe(acac)_3$, 1,2-hexadecanediol, oleic acid and oleylamine.[81] Barker *et al.*[101] studied the ripening process in a solvothermal technique and showed that the size of the nucleated nanoparticles could be varied by changing the reaction temperature, ageing time and metal precursors. Recently, the effects of organic solvents on iron oxide nanoparticles in a solvothermal method were studied.[102]

1.2.2.11 Bacterial Synthesis

In 1975, Blackmore observed that certain bacteria found in marine marsh mud tended to rapidly navigate along a specific direction due to iron rich crystals (~100 nm) forming chains in the major axis.[103] Later, it was found that an unclassified magnetotactic spirillum, when cultured in a solution containing ferric salts, precipitated uniform single-crystal spinel magnetite.[104]

1.3 Preparation of Nanofluids

Nanofluids can be prepared either *via* single (one-step) or two-step processes. The details of these two methods are presented herein.

1.3.1 Two-step Method

In a two-step method, the nanoparticles are first produced as dry powders by either a physical or chemical process, as discussed in Section 2. The prepared nanoparticles are then dispersed into a fluid with the aid of mechanical or ultrasonic agitation, high-shear mixing, homogenization, or ball milling. Nanoparticles are prepared by transition metal salt reduction,[105] ligand reduction and displacement from organometallics,[106] microwave synthesis[107] and coprecipitation.[108]

Nanoparticles have a tendency to aggregate due to their high surface area and surface activity. To overcome this, nanoparticles are often stabilized with surface active species.[109] Bonnemann *et al.*[110] developed a method for the production of palladium (Pd) particles of 2.2 nm in size *via* a chemical reduction pathway. Copper nanofluids can be prepared by dispersing Cu nanoparticles in both water and transformer oil *via* sonication in the presence of stabilizers.[111] Murshed *et al.*[23] prepared a water-based titanium dioxide (TiO_2) nanofluid *via* ultrasonic dispersion. Kim *et al.*[112] prepared

copper oxide (CuO) nanofluids by directly dispersing commercially-obtained CuO nanoparticles in ethylene glycol (EG) by sonication, without stabilizers. Multi-walled carbon nanotubes (MWCNTs) are usually prepared using a two-step method.[37,113,114] The CNTs are first synthesized *via* a pyrolysis method and then suspended in a base fluid with or without the use of a surfactant.[37,113,115,116] Lee *et al.*[35] prepared metal oxide nanoparticles (Al_2O_3, CuO) using a sol–gel method and then dispersed the obtained nanoparticles in water using a sonicator. Suresh *et al.*[117] prepared an alumina–copper hybrid powder *via* a thermochemical synthesis method followed by dispersion of the nanopowder in deionized water using sodium lauryl sulphate (SLS) as a dispersant employing an ultrasonic vibrator. A water-based silver (Ag) nanofluid was prepared *via* a two-step technique.[118] Hwang *et al.*[119] prepared carbon black in water and Ag in silicon oil nanofluids *via* a two-step method. Zinc oxide (ZnO) nanofluids have been prepared *via* a two-step technique using a magnetic stirrer.[120] Choi *et al.*[121] used zirconium dioxide (ZrO_2) bead milling in a vertical, super-fine grinding mill, for the preparation of transformer-oil-based aluminum oxide (Al_2O_3) and aluminum nitride (AlN) nanofluids using *n*-hexane as a dispersant. Water-based TiO_2 nanofluids have been prepared using a two-step method.[122] A schematic representation of a two-step method involving microwave-assisted synthesis and a direct mixing technique is shown in Figure 1.4.

1.3.2 One-step Method

In a one-step method, nanoparticle preparation and dispersion in a base fluid are conducted simultaneously.[123] A one-step process can thus be used to prepare uniformly-dispersed nanoparticles stably in a base fluid.[124] The methods used to prepare nanofluids *via* a one-step process include thermal decomposition,[125] physical vapor condensation,[32] chemical reduction[126–128] and polyol synthesis.[129]

1.3.2.1 Direct Evaporation Techniques

Akoh *et al.*[130] reported a single-step direct evaporation method for the preparation of nanofluids. Direct evaporation and condensation are used to produce stable nanofluids.[131] Choi[132] developed a 'direct-evaporation' technique involving a cylinder containing a fluid that is rotated and a source material that is vaporized in the middle of the cylinder. The vapor condenses after it comes into contact with the cooled liquid, as shown in Figure 1.5. However, the drawbacks of this technique are the requirement of low-vapor-pressure liquids and a low yield.

1.3.2.2 Chemical Reduction

Metallic nanoparticles can be prepared in various solvents.[133] Cuprous oxide nanofluids have been prepared *via* the chemical reduction of copper acetate

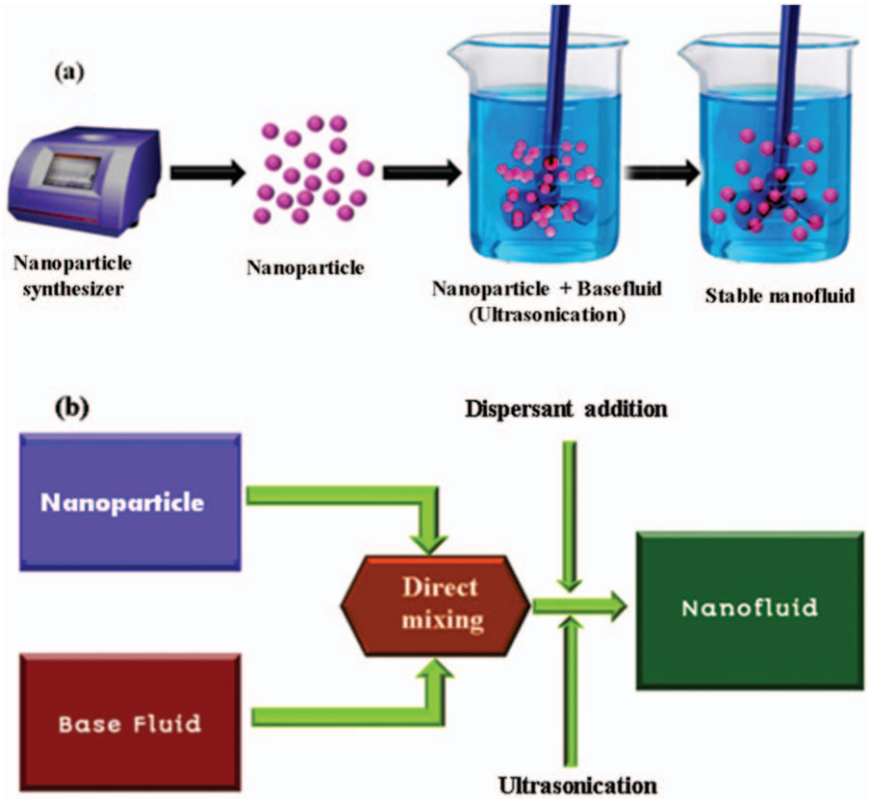

Figure 1.4 Two-step preparation process of nanofluids. (a) Nanoparticles prepared by a microwave synthesizer and particles are dispersed in a base fluid using a mechanical stirrer. (b) Direct mixing of nanoparticles followed by the addition of a dispersant and ultrasonication.

by glucose.[127] Liu *et al.*[134] prepared a water-based copper nanofluid *via* a chemical reduction method, where copper acetate was used as a precursor and hydrazine (N_2H_4) as a reducing agent. Garg *et al.*[6] synthesized copper nanoparticles *via* a chemical reduction method using water as the solvent. In this method, copper acetate was used as a precursor and sodium hydroxide as the reactant. Kumar *et al.*[128] prepared stable EG-based copper nanofluids by reducing copper sulfate pentahydrate with sodium hypophosphite as a reducing agent by means of conventional heating. Copper nanofluids were prepared *via* a routine one-step reduction method in which copper nitrate was reduced by glucose in the presence of sodium lauryl sulfate.[135] Tsai *et al.*[136] prepared aqueous gold nanofluids with different nanoparticle sizes *via* the reduction of aqueous hydrogen tetrachloroaurate ($HAuCl_4$) with tri-sodium citrate and tannic acid. Xun *et al.*[137] prepared kerosene-based silver nanofluids *via* an extraction reduction method. Said *et al.*[138] prepared

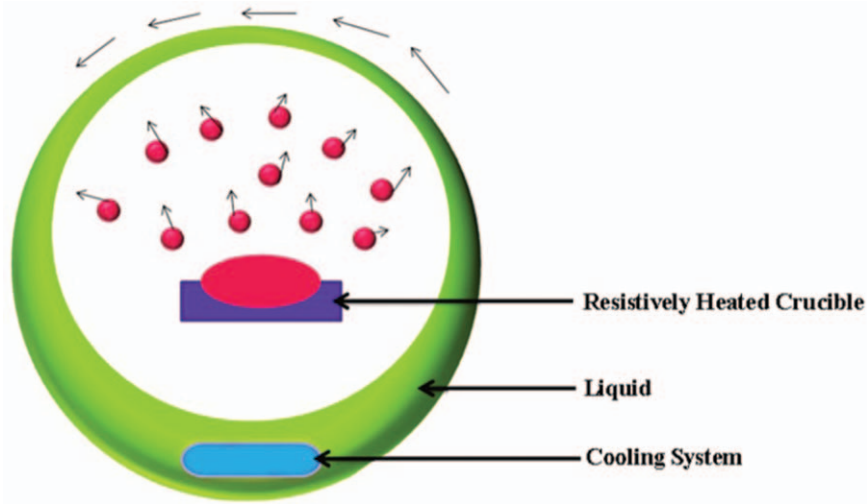

Figure 1.5 Schematic of a one-step nanofluid production system, which simultaneously produces and disperses nanoparticles in a low-vapor-pressure liquid.[147]

water-based carbon nanofibers (CNFs), functionalized carbon nanofibers (F-CNFs), reduced graphene oxide (rGO), and rGO coated over F-CNFs (F-CNFs/rGO) nanofluids using a modified Hummers' method and chemical reduction methods, as well as a hydrothermal technique. Estelle *et al.*[139] prepared reduced rGOs by chemically reducing graphene oxide using various concentrations of sodium borohydride. Santos *et al.*[140] reported the one-pot synthesis of an aqueous nanofluid with improved thermal conductivity and high colloidal stability. An aqueous nanofluid based on thioglycolic acid (TGA)-coated copper sulfide nanoparticles ($NPCu_{(2-x)}S$) was synthesized *via* a chemical reduction method.

1.3.2.3 Submerged Arc Nanoparticle Synthesis System (SANSS)

A stable CuO nanofluid was prepared using a SANSS.[141] The vaporized metal in this process undergoes nucleation, growth and condensation, resulting in nanoparticles being dispersed in deionized water. Using this approach, nanofluids containing CuO particles of 49.1 ± 38.9 nm in size were obtained.[141] EG-based nanofluids containing silver nanoparticles of 12.5 nm in size were synthesized using SANSS.[142] A schematic representation of the SANSS is shown in Figure 1.6.

1.3.2.4 Laser Ablation

Laser ablation is another single-step technique that can be used to produce and disperse nanoparticles directly in base fluids. Various nanofluids have

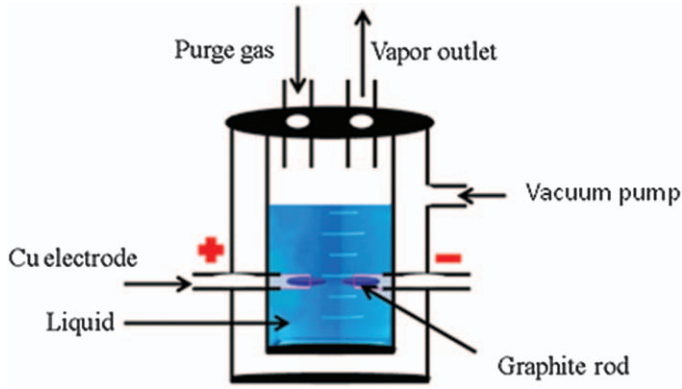

Figure 1.6 Schematic representation of the Submerged Arc Nanoparticle Synthesis System (SANSS).

been prepared *via* laser ablation methods[143–145] by ablating solid metals such as Cu, Ag, and Au submerged in a base fluid.[144] Kim *et al.*[143] prepared bare Au-water nanofluids *via* pulsed laser ablation in liquids. Lee *et al.*[144] prepared a water-based Cu nanofluid *via* a pulsed laser ablation in liquid (PLAL) method using Cu pellets. Phuoc *et al.*[145] used a multi-beam laser ablation technique for the synthesis of water-based silver nanofluids. One-step laser ablation techniques have also been used to synthesize a variety of nanofluids with different nanoparticles including such as Cu[146] and Ag.[147] Tran *et al.*[147] prepared water-based Ag and Al nanofluids with a particle size of 9–21 nm using a laser ablation technique, wherein a Nd:YAG laser was used to ablate Ag and Al in deionized water. A tin solar nanofluid was prepared *via* PLAL, wherein bulk tin immersed in EG was ablated using a femtosecond laser. It was reported that the stability and properties of the solar nanofluid was enhanced when compared to nanofluids prepared *via* conventional synthesis methods. Lee *et al.*[144] prepared a CuO nanofluid *via* PLAL using a single-pulsed laser beam ($k = 532$ nm) as follows: (1) a copper pellet was placed in a beaker filled with deionized water (DIW); (2) a Nd:YAG laser was used to produce a CuO/DIW nanofluid over 8 h. Al_2O_3 nanoparticles were synthesized using laser ablation (at different energies of 1, 3, and 5 J) using an Al target in DIW.[148] Mbambo *et al.*[149] synthesized an silver nanoparticles decorated ethylene glycol based nanofluid using a hybrid chemical–physical laser based approach, where PLAL was conducted in parallel with well-established standard vacuum pulsed laser deposition (PLD) technology to synthesize nanostructured and nanophase materials in the form of thin film coatings (LLSI/PLAL). The advantage of this approach is the combination of two major effects; namely, the standard ablation process due to the laser–matter interaction and the acoustic process caused by the explosion of the native gas bubbles during the local overheating at the target–liquid interface. Kazakevich *et al.*[150] discussed in detail the experimental setup for laser ablation in a liquid environment. A solid target placed

under a thin layer of liquid is exposed to laser radiation. Irradiation of the metal surface results in fast removal of the material and the ejected NP remains in the liquid that surrounds the target, resulting in the formation of a colloidal solution. Due to accumulation of nanoparticles in the surrounding liquid, their prolonged interaction with laser radiation is possible. Riahi *et al.*[151] prepared water-based Al_2O_3 nanofluids using a nanosecond Nd:YAG pulsed laser operating at 1064 nm. Woo *et al.*[152] prepared water-based graphite oxide (GO) nanofluids with enhanced thermal conductivity using PLAL and studied the effect of laser frequencies on the variation in the size and morphology of the GO nanoparticles. It was reported that the laser frequency significantly affects the size and morphology of the GO nanoparticles during laser ablation, leading to a profound variation in the thermophysical properties of the GO nanofluids. Maximum thermal conductivity enhancement of 82% was achieved for the nanofluids prepared at a laser frequency of 10 Hz. A comparative study on the role of the nature of the laser on nanoparticle preparation was reported by Rafique *et al.*[153] where water-based Ag nanoparticles were prepared *via* a laser ablation method using a continuous wave (CW) diode laser and a pulsed Nd:YAG laser. Vegetable oil based Ag nanofluids were prepared *via* laser ablation.[154] The target Ag was immersed in a beaker containing 55 mL of vegetable oil. The laser pulse energy/area gives the fluence that is used to prepare the nanostructures in various vegetable oils. A schematic representation of the laser ablation process is shown in Figure 1.7.

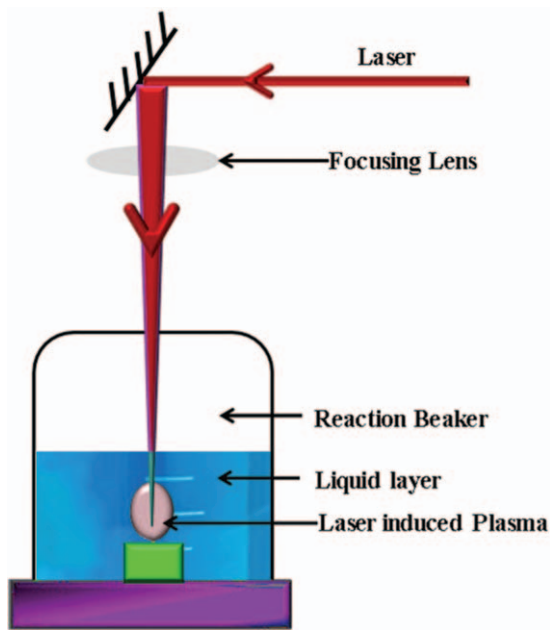

Figure 1.7 Schematic illustration of the experimental apparatus used in laser ablation.

1.3.2.5 Microwave Irradiation

Another one-step approach adopted for nanofluid synthesis is microwave irradiation.[155] Copper nanofluids have been prepared by reducing $CuSO_4 \cdot 5H_2O$ with $NaH_2PO_2 \cdot H_2O$ in EG under microwave irradiation.[156] Mineral oil (MO) based silver nanofluids have also been prepared using this method.[157] Ethanol-based silver nanofluids were prepared using a microwave-assisted one-step method.[158] Polyvinylpyrrolidone (PVP) was used as a stabilizer and reducing agent for colloidal silver in solution.[158] Seifikar *et al.*[159] synthesized a carbon quantum dots (CQDs) nanofluid *via* the microwave heating of PEG 200 (PEG 200), wherein PEG acts as a carbon source, base fluid and dispersant simultaneously. Nikam *et al.*[160] prepared CuO nanoparticles using a microwave-assisted continuous-flow synthesis technique.

1.3.2.6 Polyol Process

In the polyol process,[161,162] a metal precursor is dissolved in a liquid polyol (usually EG) to reduce the metallic precursor, followed by nucleation and growth.[161] Other one-step techniques used for nanofluid preparation are the step physical vapor condensation method[32] and plasma discharging technique.[163] Zeroual *et al.*[164] synthesized EG-based silver nanofluids *via* a polyol process. The synthesis process is based on the reduction of $AgNO_3$ in the presence of the aqueous emulsion of latex copolymer along with EG. Oliveria *et al.*[165] prepared stable EG-based diamond–silver hybrid nanofluids *via* a polyol process. The stability of the nanofluid can be attributed to the ions in the dispersion that contribute toward electrostatic stabilization, preventing the agglomeration of the nanoparticles and their sedimentation.

1.3.2.7 Phase-transfer Method

In the phase-transfer method, the reactant migrates from one phase into another phase where the reaction occurs. This method has the advantage of overcoming the problems associated with the insolubility of precursor materials in base fluids during the preparation of nanofluids.[166] Yang *et al.*[167] developed a general protocol to transfer metal ions from an aqueous solution to an organic medium. Combining phase-transfer technology with a wet chemistry method for the synthesis of nanoparticles is an effective way to prepare nanofluids.[166] A simple process based on amine chemistry for the phase-transfer of platinum nanoparticles from an aqueous to an organic solution was reported by Kumar *et al.*[168] By vigorous shaking of a biphasic mixture of platinum nanoparticles in an aqueous medium and octadecylamine (ODA) in hexane, an aqueous platinum nanoparticle complex was prepared with the ODA molecules present in the organic phase and the prepared particles are hydrophobic in nature.[168] In a similar way, gold and silver nanoparticles are transferred from the aqueous to organic phase using alkylamine as a surfactant.[169] Graphene oxide nanosheets (GONs) were

successfully transferred from water to *n*-octane after modification by oleylamine.[170] Apart from surfactants and polymers,[171] surface treatment[172] has also been used to produce stable nanofluids. However, the addition of additives can modify the surface properties of the particles, which may have a synergistic or antagonistic effect on thermal properties.

1.3.2.8 Wet Mechanochemical Techniques

Mechanical actuation that involves the top-down approach for synthesizing nanoparticles is a simple, cost-effective and environmentally benign alternative for synthesizing nanofluids. This method includes crushing, followed by milling and grinding. The enormous developments in the technique of high-energy ball milling (HEBM) have made it possible for the production of ultrafine nanoparticles of different materials.[173] Inkyo *et al.*[174] developed a bead mill process for the preparation of well-dispersed suspensions of TiO_2 (titania) nanoparticles (5%) in methyl methacrylate (MMA). TiO_2–PMMA nanocomposites were synthesized *via* subsequent polymerization of the TiO_2–MMA suspension. Harjanto *et al.*[175] prepared TiO_2–water nanofluids *via* a one-step process in which titania nanoparticles were ball-milled together with distilled water for 15 h. Nine *et al.*[176] prepared water-based copper and copper oxide nanofluids *via* ball milling in an aqueous medium. To prepare stable nanofluids, the ball milling was performed using different ball sizes (1 mm balls for 30 min and 3 mm balls for 1 h). Almasy *et al.*[177] prepared a ferrofluid (10 and 15 nm) using a vibrating ball mill. It was reported that a ferrofluid prepared *via* a wet-milled technique showed higher saturation magnetization than that of a ferrofluid suspension prepared *via* a co-precipitation synthesis.

1.3.2.9 Sol–Gel Method (Hydrolysis)

Sol–gel process is a technique widely used for the synthesis of nanofluids. There are two stages in this process, (i) hydrolysis: in this process the functional binders of the precursors are substituted with hydroxyl groups. (ii) Condensation reaction : a continuous network is formed as the hydroxyl groups of the monomers become connected.[178] For the preparation of water-based silica nanofluids using a sol–gel process, tetraethyl orthosilicate (TEOS) was taken as the precursor, ethanol as a solvent, DIW for the hydrolysis reaction, and ammonium hydroxide as a base catalyst.[179] Samed *et al.*[180] prepared stable water-based TiO_2 nanofluids using a sol–gel technique. Jing *et al.*[181] prepared water-based silica nanofluids containing different particle sizes (5, 10, 25, and 50 nm) by varying the TEOS concentration.

1.3.2.10 Emulsion Polymerization

Emulsion polymerization is a polymerization process in which emulsification of hydrophobic polymers is achieved using an emulsifier in aqueous

solution, then free radicals are generated using either water or oil soluble initiators. Goud *et al.*[182] prepared nanoencapsulated phase change materials (nEPCMs) *via* mini-emulsion polymerization. Petroleum jelly (45 g) and paraffin wax (5 g) were heated in a beaker. The composite was then mixed with AIBN, oleylamine and styrene using an ultrasonicator for 1 h at 55 °C. Triton X-100 and DIW were then added to this mixture and mixed using an ultrasonic probe for 30 min. The solution was kept under an inert atmosphere (nitrogen purging) for the polymerization process. After nitrogen purging, the solution was kept at constant temperature at 75 °C and stirred continuously using a mechanical stirrer at 400 rpm for 15 h to obtain nEPCM. Finally, a PCM nanofluid was prepared by dispersing the nEPCM in deionized water using an ultrasonic shaker. Han *et al.*[183] prepared a suspension of indium nanoparticles in polyalphaolefin (PAO) using a one-step, nanoemulsification method. An indium pellet was added to PAO oil and then the mixture was heated 20 °C above the indium melting temperature (157 °C). A PAO aminoester dispersant was injected into the reaction vessel, which also acted as a stabilizer, and the mixture was allowed to stirrer for 2 h to form an emulsion with micron-sized droplets. Then, the emulsion was exposed to high-intensity ultrasound radiation for more than 2 h until a stable nanofluid was formed. Using an emulsification and polymerization route Kim *et al.*[184] prepared biphasic nano colloids *via* the free-radical polymerization of a mixture of an acrylate copolymer precursor consisting of methyl acrylate, methyl methacrylate, and vinyl acetate which was dissolved in poly(dimethyl siloxane) (PDMS). The increasing molecular weight leads to the incompatibility of the acrylate copolymer in the PDMS and drives the phase separation on the nanometer scale and at the end of the polymerization process, with one phase partially or entirely surrounding the other phase, and the resulting structure referred to as a biphasic structure or an acorn structure due to its morphology. Joseph *et al.*[185] synthesized a polystyrene encapsulated PCM *via* a mini-emulsion polymerization. In this method, *n*-octadecane was used as PCM, styrene as the monomer for encapsulation of the PCM, α-α′ azoisobutyronitrile solution as the free radical initiator for polymerization, TritonTM X-100 as the surfactant, and oleylamine as the short-term stabilizer to protect the polymer against temperature and oxygen during the synthesis. Jitheesh *et al.*[186] prepared a composite PCM by homogeneously mixing paraffin wax and petroleum jelly to encapsulate polystyrene shells *via* a mini emulsion polymerization process, Bhanvase *et al.*[187] synthesized water-based (polyaniline) (PANI) nanofiber nanofluids *via* an ultrasound-assisted emulsion polymerization method. Yao *et al.*[188] prepared a novel functionalized microgel-based hybrid nanofluid, composed of a composite core of poly(2-dimethylamino ethyl methacrylate) microgel and silica (PDMAEMA/SiO_2) and a shell of polyetheramine, fabricated *via* the combination of inversed emulsion polymerization, biomimetic silicification and grafting approach.

1.3.2.11 Green Synthesis

Many research studies have proved that the preparation of nanofluids by green methods is more effective than traditional methods. Various physical and chemical approaches for synthesizing nanofluids impact the environment badly due to the toxic nature of chemicals. The plant-based synthesis of nanofluids is a quick and easy procedure and does not require high temperature. Green synthesis approaches can be scaled up easily in the preparation of nanoparticles and nanofluids. Green synthesis methods have attracted much attention in recent years as they include the usage of vitamins, enzymes, amino acids and plant extracts. Sarafaz *et al.*[189] prepared different volume fraction (0.1%, 0.5% and 1%) silver nanofluids (ethylene-glycol/water (50 : 50 by volume) as a base fluid) using a plant extract method from green tea leaves and silver nitrate. Kumar *et al.*[190] prepared metallic and non-metallic nanofluids from green synthesized silver and selenium nano-particles (NPs) using the Azadirachta indica plant (Neem). It has been reported that at room temperature, a low concentration of Neem leaf extract is sufficient to biosynthesize silver NPs in the lab from silver nitrate solution and selenium NPs from sodium selenite. Jameel *et al.*[191] prepared platinum nanoparticles *via* both sonochemical and conventional methods (one-pot synthesis methods), using a Prosopis farcta fruit (PFF) extract as a reducing agent and stabilizer. Rufus *et al.*[192] synthesized hematite nanoparticles using an aqueous leaf extract of Anacardium occidentale as a reducing and capping agent. It has been reported that synthesized nanoparticles enhance the thermal conductivity of conventional base fluids; water and EG at room temperature. Gautham *et al.*[193] prepared iron (Fe) nanoparticles using extracts of Terminalia bellirica (TB), Moringa oleifera fruit (MOF) and Moringa oleifera leaves. Among these, TB extract based NPs showed superior antioxidant activity when compared to the other biosynthesized Fe samples. Ranjbarzadeh *et al.*[194] prepared silica nanoparticles using a rice plant source and prepared silica nanofluids. The prepared nanofluids exhibited well-defined nanostructure and long-term stability. Okonkwo *et al.*[195] prepared silica (SiO_2) and titanium (TiO_2) nanoparticles using olive leaf extract (OLE) and barley husk (BK), respectively, and prepared water/BH–SiO_2 and water/OLE-TiO_2 nanofluids. Omiddezyani *et al.*[196] prepared a cobalt ferrite/reduced graphene oxide ($CoFe_2O_4$/rGO) nanocomposite using gallic acid (GA) as a green agent at room temperature. It was shown that π–π interactions between the graphene and the aromatic ring of GA enhanced the stability in a suspension. Sone *et al.*[197] synthesized CuO nanoparticles using *Callistemon viminalis* flower extracts at room temperature as a chelating agent and prepared water-based CuO nanofluids. Govindasamy *et al.*[198] prepared magnesium oxide nanoparticles (MONPs) using Pisonia alba leaf extract. This study reported that the MONPs showed good antioxidant and antifungal properties. Luna-Sanchez *et al.*[199] prepared silver nanoparticles using Jalapeno chili extract. The reduction of the silver nanoparticles was achieved by the flavones and flavanols present in the extract of Capsicum annuum var annuum. Sadri *et al.*[200] prepared graphene nanoplatelet

nanofluids *via* a one-pot free radical grafting method using gallic acid. It was reported that the nanofluids showed good stability even after 63 days of preparation. Sadri *et al.*[201] prepared multi-walled carbon nanotubes (MWCNTs) using a free-radical grafting reaction and dispersed them in water to form an aqueous suspension of MWCNTs. It was reported that the thermophysical properties and stability of the MWCNTs was better in aqueous suspension. Shirazi *et al.*[202] synthesized nitrogen-doped activated carbon/graphene using high nitrogen levels employing empty fruit punch pulp and formulated it into a nanofluid for the analysis of its thermoelectric properties. Pauzi *et al.*[203] prepared ZnO nanofluids using gum Arabic as a stabilizer. It was reported that the stability of the ZnO nanofluids was extended to 6 months due to the effect of gum Arabic. Hosseini *et al.*[204] prepared highly-dispersed, covalently-functionalized MWCNTs using clove extract *via* a one-pot free-radical grafting method. Then, the prepared nanotubes were dispersed in water to form nanofluids. Kulkarni *et al.*[205] synthesized silver nanoparticles using neem leaf extracts. Mostafa Yusefi *et al.*[206] prepared Fe_3O_4 nanoparticles using *Garcinia mangostana* fruit peel as a stabilizing and capping agent *via* a co-precipitation method. Zainona and Azmi prepared hybrid nanofluids by dispersing TiO_2–SiO_2 nanoparticles in water and a bio-glycol mixture. The bio-glycol based nanofluids prepared in a ratio of 40 : 60 showed good stability and enhanced thermal properties.[207] Sarafraz *et al.*[208] prepared silver nanoparticles using green tea leaf extract and the prepared nanoparticles were dispersed in coconut oil.

1.4 Enhancement of Nanofluid Stability

The long-term stability of nanofluids is an essential requirement for their applications. Unlike molecular fluids, the production of well-stabilized nanofluids is a difficult task. Particle–particle and particle–fluid interactions account for the stability of nanofluids. Owing to the high surface area-to-volume ratio of fine nanoparticles, the dispersed particles (even with stabilizing entities) have a tendency to aggregate because of van der Waals attraction forces that dominate the other repulsion forces, namely; double layer electrostatic repulsions, hydration forces and steric forces.[209,210] For the production of stable nanofluids, one has to produce fairly monodisperse nanoparticles and functionalize them with a suitable stabilizing moiety to prevent interparticle attractions. Even with the best available production route, it is difficult to produce nanoparticles with a polydispersity of $<5\%$.[211] Chemical methods (surfactant addition, pH adjustment, and surface modification) and physical methods (ultrasonic agitation, homogenization, and ball milling) have been applied to sustain the long-term stability of nanofluids.

1.4.1 Chemical Treatment Methods

From an application point of view, the stability of nanofluids is a major concern. The stability of nanofluids depends on the nature of the base

fluid and nanoparticles. By the addition of surfactants or modification of the particle surfaces, the stability of nanofluids can be improved.

1.4.1.1 Surfactant Addition

Nanofluids are thermodynamically unstable systems. However, they can be made kinetically stable with the aid of suitable surface-active species. Surfactants are widely used in nanofluids research to disperse the nanoparticles evenly in the base fluid. The type of surfactant can be selected based on the choice of the base fluid. Surfactants can be anionic (negatively charged), cationic (positively charged), non-ionic (neutral), or amphoteric (both negatively and positively charged) based on the charge on their head group. Commonly used surfactants in nanofluids research are sodium dodecyl sulfate (SDS),[212] oleic acid,[213–218] cetyl trimethyl ammonium bromide (CTAB),[219] and polyvinyl pyrrolidone (PVP).[219] Almanassra *et al.*[220] studied the effect of three different types of surfactants; gum arabic (GA), PVP, and SDS on the stability and thermo-physical properties of carbon nanotube (CNT)/water nanofluids. Choi *et al.*[221] studied the effect of various surfactants such as sodium dodecylbenzenesulfonate (SDBS), CTAB, SDS, and Triton X-100 (TX-100) on the suspension stability and solar thermal absorption characteristics of water-based nanofluids containing MWCNTs that can be used as working fluids for volumetric solar thermal receivers. Vekas *et al.*[222] prepared nano-sized particles (typically 3–15 nm particles of magnetite, maghemite or cobalt ferrite) in a magnetic nanofluid stabilized with various chain length surfactants. Das *et al.*[223] studied the effect of different surfactants (SDS, CTAB, oleic acid and acetic acid) on the stability of water-based TiO_2 nanofluids.

1.4.1.2 Surface Functionalization

In this method, the surfaces of the nanoparticles or nanotubes are functionalized before dispersing them into the base fluids. Functionalization introduces electrochemically active sites on the nanoparticle/nanotube surfaces, thus improving their dispersion in the base fluid.[224] Nanoparticles are more stable when the pH of the solution is far from the isoelectric point, at which the particles have surface charge and the zeta potential values are zero.

1.4.2 Physical Treatment Methods

In this method, high energy is applied to nanofluids through ultrasonication, homogenization or ball milling to break the nanoparticle clusters and form a well-dispersed colloidal suspension.

1.4.2.1 Ultrasonication

In this method, the liquid sample is irradiated with ultrasonic (>20 kHz) waves. Sound waves propagate in the liquid media resulting in alternating high-pressure (compression) and low-pressure (rarefaction) cycles. During rarefaction, high-intensity sonic waves create small vacuum bubbles or voids in the liquid, which then collapse violently (cavitation) during compression, creating very high local temperatures. Ultrasonication (bath or probe) is a commonly used method by which to physically disperse nanoparticle clusters. Probe sonication is the most widely employed stabilization method among the physical treatment methods. Sound energy at an ultrasonication level of 20 kHz and above is applied for a predetermined period of time to disperse nanoparticles into a base fluid and to break clusters of nanoparticles.[225] Mahbubul *et al.*[226] studied the influence of ultrasonication time on the stability of a water-based Al_2O_3 nanofluid. Garg *et al.*[227] investigated the effect of ultrasonication time (20 min, 40 min, 60 min, and 80 min) on the viscosity and heat transfer performance of a MWCNT nanofluid. Kwak and Kim *et al.*[228] studied the effect of ultrasonication time for different time periods from 1 h to 30 h on EG-based CuO nanofluids. Lee *et al.*[229] stabilized water-based Al_2O_3 nanofluids by applying ultrasonic vibration (5 h, 20 h and 30 h) at sound frequencies of 30–40 kHz. The influence of varying the sonication time on the stability of CuO–water nanofluids was studied and reported by Nemade *et al.*[230]

1.4.2.2 Ball Milling

This is a process where micron-sized materials are reduced to ultrafine powders. In a ball mill, the size reduction is achieved by impact and attrition, where a hollow cylindrical shell rotates about its axis either horizontally or at a slight angle and is partially filled with balls made of steel or stainless steel.[231] The collision between the tiny rigid balls in the cylinder generates localized high pressure. Farbod *et al.*[232] synthesized engine oil-based CuO nanofluids, wherein oil, nanoparticles and grinding balls were put into a container and milled for 3 h by a planetary mill.

1.5 Techniques for Characterizing Nanofluids

It is necessary and important to understand the physicochemical properties of prepared nanoparticles and nanofluids. For this purpose, there are a wide range of characterization techniques, such as X-ray diffraction (XRD), phase contrast microscopy, and transmission electron microscopy (TEM), which are used to gain information on nanoparticle size, shape, composition and porosity. In this section, the basic characterization techniques are discussed in detail.

1.5.1 XRD

This is one of the most extensively used techniques for the characterization of nanoparticles of any size. Since the wavelengths of X-rays are similar to the size of atoms, they are useful for determining crystal structures, the nature of phases, lattice parameters and crystalline grain size, achieved using XRD.[233] The principles of crystallography are based on Bragg's law. The Scherrer equation is used to determine crystallite size. For spherical particles the equation for crystallite size can be written as:

$$d = \frac{0.89\lambda}{\beta \mathrm{Cos}\theta_{\max}} \tag{1.1}$$

where d is the crystallite size of the particles, 0.89 is a proportionality constant for spherical particles; β is the full width at half maxima, θ is the angle of diffraction and λ is the wavelength of the X-ray source (for CuKα, $\lambda = 1.5416$ Å).

1.5.2 Dynamic Light Scattering (DLS)

DLS, also referred to as quasi-elastic light scattering (QELS), is a non-invasive technique for measuring the hydrodynamic size and size distribution of molecules and particles typically in the submicron range.[234] Typical applications of DLS are the characterization of particles or molecules that have been dispersed in a liquid. The Brownian motion of the particles or molecules in suspension causes laser light to be scattered at different intensities. Analysis of these intensity fluctuations yields the velocity of the Brownian motion and the particle size can be calculated using the Stokes–Einstein equation. In light scattering experiments, a monochromatic light source, usually a laser, passes through a polarizer and onto the sample. The scattered light then goes through a second polarizer where it is collected by a photomultiplier tube (PMT). The instantaneous scattered field can be regarded as the superposition of waves scattered from the individual scattering centers. The scattered electric field at a given scattering wave vector q is expressed as:

$$E(q,t)\alpha \sum_{j=1}^{N} \exp\left(i\vec{q} \cdot \vec{r}_j(t)\right) \tag{1.2}$$

where $\vec{r}(t)$ is the center-of-mass position of the jth scatterer. The scattered field given by eqn (1.2) therefore fluctuates in response to the motions of the scatterers. If the fluctuations are faster than 10^{-6} s, a filter method is used to detect and analyze the timescale of these fluctuations. Optical mixing or beating methods are usually used for processes that occur on timescales slower than about 10^{-6} s. In optical mixing methods, no "filter" is inserted between the scattering medium and the detector (PMT). The scattered light impinges directly on the PMT cathode. In the homodyne (self-beat) method

only the scattered light impinges on the photocathode, while in the heterodyne method a local oscillator (a small portion of the unscattered laser beam) is mixed with the scattered light on the cathode surface. Since PMT is a square-law detector, its instantaneous current output is proportional to the square of the incident electric field $I(t) \propto \|E(t)\|^2$. The PMT output is fed to a digital correlator, which calculates the intensity–intensity auto correlation function (also known as homodyne correlation function), which is defined as:

$$\langle I(q,0)I(q,t)\rangle = B\left\langle |E(q,0)|^2 |E(q,t)|^2 \right\rangle \tag{1.3}$$

where B is the proportionality constant. The normalized intensity auto-correlation function, $g^{(2)}(q,t)$, is defined as:

$$g^{(2)}(q,t) = \frac{\langle I(q,0)I(q,t)\rangle}{\langle I(q)\rangle^2} \tag{1.4}$$

and the normalized electric field auto-correlation function (also known as the heterodyne correlation function) is defined as:

$$g^{(1)}(q,t) = \frac{\langle E(q,0)E(q,t)\rangle}{\langle |E(q)|\rangle^2} \tag{1.5}$$

with the assumption that the scattering volume can be divided into a large number of statistically independent sub-regions and the scattered electric field is a Gaussian random variable, $g^{(2)}(q,t)$, related to $g^{(1)}(q,t)$ by:

$$g^{(2)}(q,t) = 1 + \beta \left| g^{(1)}(q,t) \right|^2 \tag{1.6}$$

The above equation is known as the Siegert relation and the constant β depends on the coherence area set by the optics of the instrument and is obtained by fitting. The heterodyne correlation function, $g^{(1)}(q,t)$, which is related to the position of the particles, can be redefined as the intermediate scattering function (dynamic structural factor), $F(q,t)$, using eqn (1.7):

$$F(q,t) \alpha \langle E(q,0)E(q,t)\rangle \tag{1.7}$$

$$F(q,t) = \frac{1}{N} \sum_{I=1}^{N} \sum_{J=1}^{N} \left\langle \exp\left(i\, q . \left[\vec{r}_i(0) - \vec{r}_j(t) \right] \right) \right\rangle \tag{1.8}$$

hence,

$$g^{(1)}(q,t) = \frac{F(q,t)}{S(q)} \tag{1.9}$$

where, $S(q) = F(q,0)$. For an non-interacting suspension, $S(q) = 1$, by measuring $g^{(1)}(q,t)$ (either using a homodyne or heterodyne method), one can determine the self-diffusion coefficient, D_0, of the colloidal particles.

1.5.3 TEM

TEM is a technique that uses an electron beam to image a nanoparticle, providing much higher resolution than is possible using light-based imaging techniques such as optical microscopy.[235] TEM also provides information on nanoparticle size, grain size, size distribution, and morphology. TEM exploits three different electron beam–specimen interactions, *i.e.*, un-scattered electrons (transmitted beam), elastically scattered electrons (diffracted beam) and inelastically scattered electrons. The intensity of the transmitted electrons is inversely proportional to the specimen thickness. Areas of the specimen that are thicker will have fewer transmitted electrons and so will appear darker; conversely the thinner areas will appear lighter due to more transmission. The scattered part of the incident beam is transmitted through the remaining portions of the specimen. All incident electrons have the same energy and enter the specimen normal to its surface. All incidents that are scattered by the same atomic spacing will be scattered by the same angle. These scattered electrons can be collimated using magnetic lenses to form a pattern of spots, with each spot corresponding to a specific atomic spacing (a plane). This pattern can then yield information about the orientation, atomic arrangements and phases present in the specimen. Also, incident electrons can interact with the specimen inelastically and lose their energy during the interaction. These electrons are then transmitted through the rest of the specimen.[236]

Typically, a TEM consists of three stages of lensing[235] comprising condenser, objective, and projector lenses. The condenser lenses are responsible for primary beam formation, whilst the objective lenses focus the beam that comes through the sample itself (in scanning TEM (STEM) mode, there are also objective lenses above the sample to make the incident electron beam convergent). The projector lenses are used to expand the beam onto a phosphor screen or other imaging device, such as a film. The magnification of the TEM is due to the ratio of the distances between the specimen and the image plane of the objective lens. Additional quad or hexapole lenses allow for the correction of asymmetrical beam distortions, known as astigmatism. It should be noted that TEM optical configurations differ significantly with implementation, with manufacturers using custom lens configurations, such as in spherical aberration corrected instruments or TEMs that utilize energy filtering to correct electron chromatic aberration.

1.5.4 Zeta Potential Measurements

Zeta potential measurements provide information about the surface charge of nanoparticles dispersed in solution. Hence, zeta potentials play a significant role in stabilizing particle suspensions (short- and long-term stability). When a charged particle is introduced into a polar medium, the depletion of co-ions (ions with the same charge as the particle surface)

from the surface and the adsorption of counter ions (ions with the opposite charge to the particle surface) occurs.[58] The development of a net charge at the particle surface through ionization or by dissociation of surface groups affects the distribution of ions in the surrounding interfacial region, resulting in an increased concentration of counter ions (ions of opposite charge to that of the particles) close to the surface. Whatever the charging mechanism, the final surface charges of the co-ions are balanced by an equal but oppositely-charged region of counterions. Some of the counterions are bound, usually transiently to the surface within the so called *Stern layer* or *Helmholtz layer*, while other ions form an atmosphere of ions in rapid thermal motion close to the surface, known as the diffuse electrical double layer, as shown in Figure 1.8a. The difference between the bound and free ions in the diffuse layer is analogous to the difference between a water molecule in a sea and in the atmosphere.[237] Within the diffuse layer there is a notional boundary inside which the ions and particles form a stable entity. When a particle moves (*e.g.*, due to gravity), ions within the boundary move with it, but any ions beyond the boundary do not travel with the particle. This boundary is called the surface of hydrodynamic shear or slipping plane. The potential that exists at this boundary is known as the zeta potential, as shown in Figure 1.8b.

The magnitude of the zeta potential gives an indication of the potential stability of the colloidal system. If all the particles in a suspension have a large negative or positive zeta potential then they will tend to repel each other and there will be no tendency to flocculate. However, if the particles have low zeta potential values then there is no force to prevent the particles coming together and flocculating. The general dividing line between stable and unstable suspensions is $+30$ mV or -30 mV. Particles with zeta potentials above ± 30 mV are normally considered stable[238] (Figure 1.8c). However, if the particles have a large density that is different from the dispersant, they will eventually sediment.[238] The important factors affecting the zeta potential are pH, conductivity and concentration of formulations.

Zeta potential measurements can be conducted using an electrophoresis approach. When an electric field is applied across an electrolyte, charged particles suspended in the electrolyte are attracted towards the electrode of opposite charge, as shown in Figure 1.8d, where the viscous forces acting on the particles tend to oppose this movement. When equilibrium is reached between these two opposing forces, the particles move with a constant velocity. The velocity of the particle is dependent on the strength of the electric field or voltage gradient, the dielectric constant of the medium, the viscosity of the medium and the zeta potential. The velocity of a particle in an electric field is referred to as its electrophoretic mobility, which is related to the zeta potential by the Henry equation:

$$U_{\mathrm{E}} = \frac{2\varepsilon\zeta f(ka)}{3\eta} \tag{1.10}$$

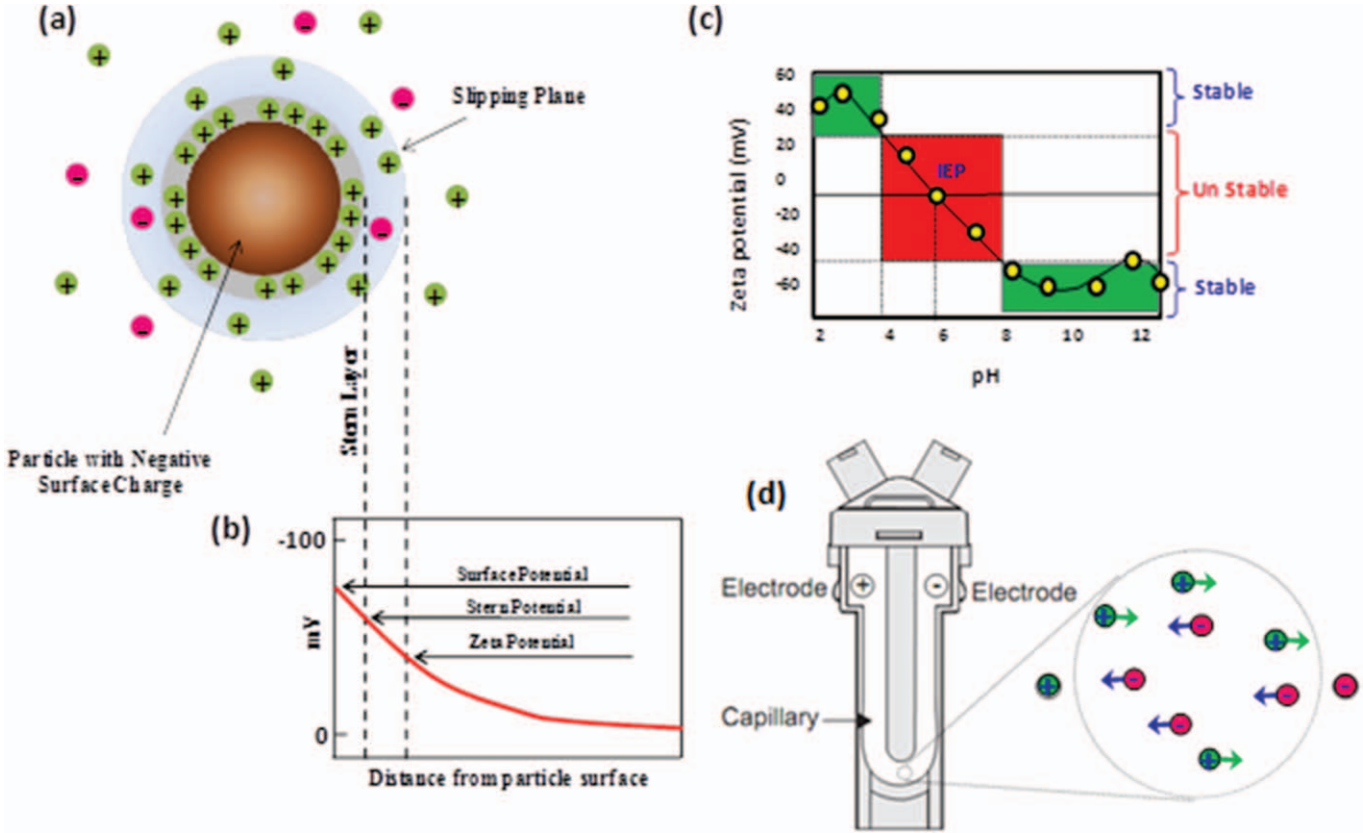

Figure 1.8 Schematic representation of (a) a charged particle with an electric double layer, (b) the distance from the particle surface and the corresponding potentials, (c) a typical plot of the zeta potential *versus* pH showing the position of the isoelectric point and the pH values where the dispersion is stable and unstable, and the (d) electrophoretic mobility in a folded capillary cell.

where, U_E is the electrophoretic mobility, ζ is the zeta potential, ε is the dielectric constant, η is the viscosity and $f(ka)$ is Henry's function ($\approx$1.5 by *Smoluchowski* approximation for a particle larger than 0.2 μm dispersed in electrolyte containing more than 10^{-3} molar salt). For small particles in low dielectric constant media $f(ka)$ becomes 1 *via* the Huckel approximation for non-aqueous measurements. κ is the inverse Debye length, and κ^{-1} is often taken as being a measure of the ''thickness'' of the electrical double layer.

For zeta potential measurements, the laser light source is split to provide an incident and reference beam. The incident laser beam passes through the center of the sample cell, and the scattered light is detected at an angle of 17°. When an electric field is applied to the cell, any particles moving through the measurement volume will cause the intensity of light detected to fluctuate with a frequency proportional to the particle speed, and this information is passed to a digital signal processor and then to a computer. The Zetasizer Nano software produces a frequency spectrum from which the electrophoretic mobility and hence zeta potential is calculated. The intensity of the detected scattered light must be within a specific range for the detector to successfully measure it, which is achieved using an attenuator. To correct for any differences in the cell wall thickness and dispersant refraction, compensation optics are installed to maintain optimum alignment.[239]

1.5.5 Phase Contrast Optical Microscopy

Phase contrast microscopy is a very useful technique that is used to look at the aggregation of nanoparticles in nanofluids. However, the limitation of this technique is that it can only measure aggregates of fairly larger sizes (>200 nm). In phase contrast optical microscopy, a phase object causes a small phase shift in the light passing through a transparent specimen, which is then converted into amplitude or contrast changes in the image. As light travels through a medium other than a vacuum, interaction with the medium causes amplitude and phase changes that depend on the properties of the medium. The basic principle to make phase changes visible in phase contrast microscopy is to separate the illuminating background light from the specimen scattered light, which makes up the foreground details, and to manipulate these differently. The ring-shaped illuminating light that passes through the condenser annulus is focused on the specimen by the condenser. Some of the illuminating light is scattered by the specimen. The remaining light is unaffected by the specimen and forms the background light. When observing an unstained biological specimen, the scattered light is weak and typically phase-shifted by −90°, relative to the background light. This leads to the foreground and the background having almost the same intensity, resulting in a low image contrast. For a phase contrast microscope, the image contrast can be improved in two steps. The background light is phase-shifted by −90° by passing it through a phase shift ring. This eliminates the phase difference between the background and the scattered light,

leading to an increased intensity difference between the foreground and background. To further increase the contrast, the background is dimmed by a gray filter ring. Some of the scattered light will be phase-shifted and dimmed by the rings. However, the background light is affected to a much greater extent, which leads to a phase contrast effect. The above describes negative phase contrast. In its positive form, the background light is instead phase-shifted by $+90^{\circ}$. The background light will thus be 180° out of phase relative to the scattered light. This results in the scattered light being subtracted from the background light to form an image where the foreground is darker than the background. The performance of modern phase contrast microscopes is so refined that it enables specimens containing very small internal structures, or even just a few protein molecules, to be detected when the technology is coupled to electronic enhancement and post-acquisition image processing instruments.

1.5.6 Fourier-transform Infrared (FT-IR) Spectroscopy

FT-IR spectroscopy is a technique that is used to obtain insight into the nature of adsorption of functional groups at the particle interface. In FT-IR spectroscopy, the preferred IR spectroscopy method, IR radiation is passed through a sample. Some of the IR radiation is absorbed by the sample and some of it is transmitted. The resulting spectrum represents the molecular absorption and transmission, creating a molecular fingerprint of the sample. Like a human fingerprint, no two unique molecular structures produce the same IR spectrum, making IR spectroscopy useful for several types of analysis. The total internal energy of a molecule in a first approximation is the sum of its rotational, vibrational and electronic energy levels. In IR spectroscopy the interactions between matter and electromagnetic (EM) fields in the IR region is studied, where the EM waves mainly couple with the molecular vibrations. In other words, the excitation of molecules to a higher vibrational state occurs upon absorbing IR radiation. In FTIR spectroscopy studies, a small amount of solid sample is mixed thoroughly with potassium bromide in a 1 : 100 ratio (by weight) and the mixture is then compressed into a thin transparent pellet using a hydraulic press. These pellets are transparent to IR radiation and are used for analysis. If the photon energy coincides with the vibrational energy levels of the molecule the frequency is absorbed by the molecule. Hence, IR spectroscopy is a very powerful technique that provides fingerprint information on the chemical composition of the sample.

1.5.7 Thermogravimetric Analysis (TGA) and Differential Scanning Calorimetry (DSC)

TGA is a technique widely used to evaluate the amount of surfactant adsorbed on a particle surface. Specific heat capacity is a materials property

that describes the energy required to induce a change in the temperature of a unit mass of the material. DSC is used to measure this quantity. The specific heat capacity, C_p is measured using DSC by heating a sample and measuring the temperature difference between the sample and a reference. The sample material is subjected to a linear temperature program, and the heat flow rate into the sample is continuously measured, which is proportional to the instantaneous specific heat of the sample. Reference and sample crucibles are placed on a sample holder inside a furnace, which generates heat radially toward the center. Thermocouples in contact with each crucible measure the temperature. One thermoelement is shared between the crucibles allowing the temperature difference to be measured as a voltage.

1.6 Conclusion

This chapter gives an overview of nanoparticles, nanofluids and the different techniques used to prepare nanoparticles, which include top-down approaches such as mechanical milling, etching, laser ablation, electro explosion, and bottom-up approaches such as precipitation, solvothermal, flow injection, decomposition of metal carbonyls, reverse micelle, electrodeposition, sol–gel, mechanochemical, hydrothermal, and bacterial synthesis techniques. This is followed by techniques used for the preparation of nanofluids *via* two-step and single-step methods. The direct evaporation technique, chemical reduction method, submerged arc nanoparticle synthesis method, laser ablation, microwave irradiation, polyol process, phase-transfer method, wet mechanochemical technique, sol–gel method (hydrolysis), emulsion-polymerization, and green synthesis are presented in detail. The stability issues of nanofluids are discussed, along with approaches used to improve the stability of nanofluids. Methods to enhance the stability of nanofluids using chemical treatment methods (surfactant addition and surface functionalization) and physical treatment methods (ultrasonication and ball milling) are discussed in detail. Various experimental techniques used for the characterization of nanomaterials and nanofluids are also detailed. Details of XRD, DLS, TEM, zeta potential measurements, phase contrast microscopy, FT-IR spectroscopy, TGA and DSC are presented for freshers who intend to begin research on this topic.

Acknowledgements

J. P. thanks Dr R. Divakar for his support.

References

1. G. Schmid, *Nanoparticles: From Theory to Application*, Wiely-VCH Verlag GmbH & Co., Weinheim, 2004.
2. B. Bhushan, *Springer Handbook of Nanotechnology*, Spinger, New York, 2004.

3. J. Philip, P. D. Shima and B. Raj, *Nanotechnology*, 2008, **19**, 305706.
4. N. R. Karthikeyan, J. Philip and B. Raj, *Mater. Chem. Phys.*, 2008, **109**, 50.
5. P. E. Gharagozloo, J. K. Eaton and K. E. Goodson, *Appl. Phys. Lett.*, 2008, **93**, 103110.
6. J. Garg, B. R. Poudel, M. Chiesa, J. B. Gordon, J. J. Ma, J. B. Wang, Z. F. Ren, Y. T. Kang, H. Ohtani, J. Nanda, G. H. McKinley and G. Chen, *J. Appl. Phys.*, 2008, **103**, 074301.
7. B. Wright, D. Thomas, H. Hong, L. Groven, J. Puszynski, E. Duke, X. Ye and S. Jin, *Appl. Phys. Lett.*, 2007, **91**, 173116.
8. E. V. Timofeeva, A. N. Gavrilov, J. M. McCloskey, Y. V. Tolmachev, S. Sprunt, L. M. Lopatina and J. V. Selinger, *Phys. Rev. E*, 2007, **76**, 061203.
9. J. Philip, P. D. Shima and B. Raj, *Appl. Phys. Lett.*, 2007, **91**, 203108.
10. C. H. Li and G. P. Peterson, *J. Appl. Phys.*, 2007, **101**, 044312.
11. S. P. Jang, J. H. Lee, K. S. Hwang and S. U. S. Choi, *Appl. Phys. Lett.*, 2007, **91**, 243112.
12. J. Eapen, W. C. Williams, J. Buongiorno, L. W. Hu, S. Yip, R. Rusconi and R. Piazza, *Phys. Rev. Lett.*, 2007, **99**, 095901.
13. X. Zhang, H. Gu and M. Fujii, *J. Appl. Phys.*, 2006, **100**, 044325.
14. B. Yang and Z. H. Han, *Appl. Phys. Lett.*, 2006, **89**, 083111.
15. R. Rusconi, E. Rodari and R. Piazza, *Appl. Phys. Lett.*, 2006, **89**, 261916.
16. S. M. S. Murshed, K. C. Leong and C. Yang, *J. Phys. D: Appl. Phys.*, 2006, **39**, 5316.
17. S. J. Kim, I. C. Bang, J. Buongiorno and L. W. Hu, *Appl. Phys. Lett.*, 2006, **89**, 153107.
18. K. S. Hong, T. K. Hong and H. S. Yang, *Appl. Phys. Lett.*, 2006, **88**, 031901.
19. W. Evans, J. Fish and P. Keblinski, *Appl. Phys. Lett.*, 2006, **88**, 093116.
20. J. Buongiorno, *ASME J. Heat Transfer*, 2006, **128**, 240.
21. P. B. Abdallah, *Appl. Phys. Lett.*, 2006, **89**, 113117.
22. R. Prasher, P. Bhattacharya and P. E. Phelan, *Phys. Rev. Lett.*, 2005, **94**, 025901.
23. S. M. S. Murshed, K. C. Leong and C. Yang, *Int. J. Therm. Sci.*, 2005, **44**, 367.
24. T. K. Hong, H. S. Yang and C. J. Choi, *J. Appl. Phys.*, 2005, **97**, 064311.
25. D. W. Zhou, *Int. J. Heat Mass Transfer*, 2004, **47**, 3109.
26. D. Wen and Y. Ding, *Int. J. Heat Mass Transfer*, 2004, **47**, 5181.
27. S. P. Jang and S. U. S. Choi, *Appl. Phys. Lett.*, 2004, **84**, 4316.
28. P. Bhattacharya, S. K. Saha, A. Yadav, P. E. Phelana and R. S. Prasher, *J. Appl. Phys.*, 2004, **95**, 6492.
29. Q. Z. Xue, *Phys. Lett. A*, 2003, **307**, 313.
30. H. E. Patel, S. K. Das, T. Sundararajan, A. S. Nair, B. George and T. Pradeep, *Appl. Phys. Lett.*, 2003, **83**, 2931.
31. S. K. Das, N. Putra, P. Thiesen and W. Roetzel, *ASME J. Heat Transfer*, 2003, **125**, 567.

32. J. A. Eastman, S. U. S. Choi, S. Li, W. Yu and L. J. Thompson, *Appl. Phys. Lett.*, 2001, **78**, 718.
33. Y. Xuan and W. Roetzel, *Int. J. Heat Mass Transfer*, 2000, **43**, 3701.
34. H. Younes, G. Christensen, X. Luan, H. Hong and P. Smith, *J. Appl. Phys.*, 2012, **111**, 064308.
35. S. Lee, S. U. S. Choi, S. Li and J. A. Eastman, *ASME J. Heat Transfer*, 1999, **121**, 280.
36. S. U. S. Choi, Z. G. Zhang, W. Yu, F. E. Lockwood and E. A. Grulke, *Appl. Phys. Lett.*, 2001, **79**, 2252.
37. H. Xie, H. Lee, W. Youn and M. Choi, *J. Appl. Phys.*, 2003, **94**, 4967.
38. P. D. Shima, J. Philip and B. Raj, *Appl. Phys. Lett.*, 2010, **97**, 153113.
39. P. Keblinski, S. R. Phillpot, S. U. S. Choi and J. A. Eastman, *Int. J. Heat Mass Transfer*, 2002, **45**, 855.
40. J. Philip and P. D. Shima, *Adv. Colloid Interface Sci.*, 2012, **183–184**, 30.
41. R. Taylor, S. Coulombe, T. Otanicar, P. Phelan, A. Gunawan, W. Lv, G. Rosengarten, R. Prasher and H. Tyagi, *J. Appl. Phys.*, 2013, **113**, 011301.
42. R. E. Rosenzweig, *Ferrohydrodynamics*, Cambridge University Press, Cambridge, 1985.
43. G. Puliti, S. Paolucci and M. Sen, *Appl. Mech. Rev.*, 2011, **64**, 030803.
44. J. Philip, P. D. Shima and B. Raj, *Appl. Phys. Lett.*, 2008, **92**, 043108.
45. M. J. Kao, C. H. Lo, T. T. Tsung, Y. Y. Wu, C. S. Jwo and H. M. Lin, *J. Alloys Compd.*, 2007, **134–435**, 672.
46. W. Yu and H. Xie, *J. Nanomater.*, 2012, **2012**, 1.
47. B. Dudda and D. Shin, *Int. J. Therm. Sci.*, 2013, **69**, 37.
48. O. Mahian, A. Kianifar, S. A. Kalogirou, I. Pop and S. Wongwises, *Int. J. Heat Mass Transfer*, 2013, **57**, 582.
49. D. Yang, F. Yang, J. Hu, J. Long, C. Wang, D. Fu and Q. Ni, *Chem. Commun.*, 2009, 4447.
50. V. Mahendran and J. Philip, *NDT&E Int.*, 2013, **60**, 100.
51. R. A. Taylor, T. Otanicar and G. Rosengarten, *Light Sci. Appl.*, 2012, **1**, 1.
52. R. Hernández, in *POLYSOLVAT-9, 9th International IUPAC Conference on Polymer-Solvent Complexes & Intercalates*, Ukraine, 2012.
53. K. Raj and R. Moskowitz, *J. Magn. Magn. Mater.*, 1990, **85**, 233.
54. P. D. Shima, J. Philip and B. Raj, *J. Phys. Chem. C*, 2010, **114**, 18825.
55. S. Vinod and J. Philip, *J. Mol. Liq.*, 2018, **257**, 1.
56. V. Mahendran and J. Philip, *Appl. Phys. Lett.*, 2012, **100**, 073104.
57. B. B. Lahiri, S. Ranoo, A. W. Zaibudeen and J. Philip, *J. Magn. Magn. Mater.*, 2017, **441**, 310.
58. V. Mahendran and J. Philip, *Sens. Actuators, B*, 2013, **185**, 488.
59. M. Nandy, B. B. Lahiri and J. Philip, *Sens. Actuators, A*, 2020, **314**, 112220.
60. A. W. Zaibudeen and J. Philip, *Sens. Actuators, B*, 2018, **255**, 720.
61. B. B. Lahiri, S. Ranoo and J. Philip, *Infrared Phys. Thecnol.*, 2017, **80**, 71.
62. S. Ranoo, B. B. Lahiri and J. Philip, *J. Magn. Magn. Mater.*, 2020, **498**, 166138.

63. C. Anushree and J. Philip, *Colloids Surf., A*, 2019, **567**, 193.
64. T. Muthukumaran and J. Philip, *Colloids Surf., A*, 2021, **610**, 125755.
65. F. Bozon-Verduraz, F. Fiévet, J.-Y. Piquemal, R. Brayner, K. E. Kabouss, Y. Soumare, G. Viau and G. Shafeev, *Braz. J. Phys.*, 2009, **39**, 134.
66. J. S. Benjamin, *Metall. Trans. B*, 1970, **1**, 2943.
67. J. F. d. Carvalho, S. N. d. Medeiros, M. A. Morales, A. L. Dantas and A. S. Carriço, *Appl. Surf. Sci.*, 2013, **275**, 84.
68. N. Salah, S. S. Habib, Z. H. Khan, A. Memic, A. Azam, E. Alarfaj, N. Zahed and S. Al-Hamedi, *Int. J. Nanomed.*, 2011, **6**, 863.
69. A. E. D. Mahmoud, A. Stolle and M. Stelter, *ACS Sustain. Chem. Eng.*, 2018, **6**, 6358.
70. Q. Li, M. Rellán-Piñeiro, N. Almora-Barrios, M. Garcia-Ratés, I. N. Remediakis and N. López, *Nanoscale*, 2017, **9**, 13089.
71. W. Cheng, W. Zhang, L. Hu, W. Ding, F. Wu and J. Li, *RSC Adv.*, 2016, **6**, 15900.
72. J. S. Duque, M. B. Madrigal, H. Riascos and Y. P. Avila, *Colloids Interfaces*, 2019, **3**, 25.
73. V. Amendola and M. Meneghetti, *Phys. Chem. Chem. Phys.*, 2009, **11**, 3805.
74. R. A. Ismail, G. M. Sulaiman, S. A. Abdulrahman and T. R. Marzoog, *Mater. Sci. Eng., C*, 2015, **53**, 286.
75. P. Sen, J. Ghosh, A. Abdullah and K. Prashant, *Chem. Sci.*, 2003, **115**, 499.
76. J. Berasategi, A. Gomez, M. M. Bou-Ali, J. Gutiérrez, J. M. Barandiarán, I. V. Beketov, A. P. Safronov and G. V. Kurlyandskaya, *Struct. Smart Mater. Struct.*, 2018, **27**, 045011.
77. J. W. Mullin and M. M. Osman, *Cryst. Res. Technol.*, 1973, **8**, 471.
78. A.-H. Lu, E. L. Salabas and F. Schuth, *Angew. Chem., Int. Ed.*, 2007, **46**, 1222.
79. M. A. Willard, L. K. Kurihara, E. E. Carpenter, S. Calvin and V. G. Harris, *Encyclopedia of Nanoscience and Nanotechnology*, American Scientific Publishers, Valencia, CA, 2004, vol. 1.
80. S. Sun and H. Zeng, *J. Am. Chem. Soc.*, 2002, **124**, 8204.
81. S. Sun, H. Zeng, D. B. Robinson, S. Raoux, P. M. Rice, S. X. Wang and G. Li, *J. Am. Chem. Soc.*, 2004, **126**, 273.
82. D. Chen and R. Xu, *Mat. Res. Bull.*, 1998, **33**, 1015.
83. Z. Li, Q. Sun and M. Gao, *Angew. Chem., Int. Ed.*, 2005, **44**, 123.
84. F. Q. Hu, L. Wei, Z. Zhou, Y. L. Ran, Z. Li and M. Y. Gao, *Adv. Mater.*, 2006, **18**, 2553.
85. G. S. Alvarez, M. Muhammed and A. A. Zagorodni, *Chem. Eng. Sci.*, 2006, **61**, 4625.
86. R. S. Chaurasiy and H. U. Hebbar, in *Nanoscience in Food and Agriculture 4*, Springer, Cham, 2017, p. 181.
87. S. Rana, J. Philip and B. Raj, *Mater. Chem. Phys.*, 2010, **124**, 264.
88. M. Ueda, H. Dietz, A. Anders, H. Kneppe, A. Meixner and W. Plieth, *Electrochim. Acta*, 2002, **48**, 377.

89. S. Banerjee, S. Roy, J. W. Chen and D. Chakravorty, *J. Magn. Magn. Mater.*, 2000, **219**, 45.
90. C. Burda, X. Chen, R. Narayanan and M. A. El-Sayed, *Chem. Rev.*, 2005, **105**, 1025.
91. B. L. Cushing, V. L. Kolesnichenko and C. J. O'Connor, *Chem. Rev.*, 2004, **104**, 3893.
92. J. W. Long, M. S. Logan, C. P. Rhodes, E. E. Carpenter, R. M. Stroud and D. R. Rolison, *J. Am. Chem. Soc.*, 2004, **126**, 16879.
93. J. Jin, S. Ohkoshi and K. Hashimoto, *Adv. Mater.*, 2004, **16**, 48.
94. T. Tsuzki and P. G. Mccormick, *J. Mater. Sci.*, 2004, **9**, 5143.
95. J. Ding, T. Tsuzuki and P. G. M. Cormick, *J. Magn. Magn. Mater.*, 1998, **177–181**, 931.
96. P. Druska, U. Steinike and V. Šepelák, *J. Solid State Chem.*, 1999, **146**, 13.
97. H. Yang, X. Zhang, W. Ao and G. Qiu, *Mater. Res. Bull.*, 2004, **39**, 833.
98. H. Yang, X. Zhang, C. Huang, W. Yang and G. Qiu, *J. Phys. Chem. Solids*, 2004, **65**, 1329.
99. J. Wang, C. Zeng, Z. Peng and Q. Chen, *Phys. B*, 2004, **349**, 124.
100. D. E. Zhang, X. J. Zhang, X. M. Ni, H. G. Zheng and D. D. Yang, *J. Magn. Magn. Mater.*, 2005, **292**, 79.
101. A. J. Barker, B. Cage, S. Russek, R. Garg, R. Shandas and C. R. Stoldt, American Society of Mechanical Engineers, 2005, p. 581.
102. S. Chaianansutcharit, O. Mekasuwandumrong and P. Praserthdam, *Cryst. Growth Des.*, 2006, **6**, 40.
103. R. Blackmore, *Science*, 1975, **190**, 377.
104. R. B. Frankel, R. P. Blakemore and R. S. Wolfe, *Science*, 1979, **203**, 1355.
105. D. L. V. Hyning, W. G. Klemperer and C. F. Zukoski, *Langmuir*, 2001, **17**, 3128.
106. Y. Chen, X. Luo, G.-H. Yue, X. Luo and D.-L. Peng, *Mat. Chem. Phys.*, 2009, **113**, 412.
107. S. S. Pati, V. Mahendran and J. Philip, *J. Nanofluids*, 2013, **2**, 94.
108. G. Gnanaprakash, S. Mahadevan, T. Jayakumar, P. K. Sundaram, J. Philip and B. Raj, *Mater. Chem. Phys.*, 2007, **103**, 168.
109. R. Prasher, P. E. Phelan and P. Bhattacharya, *Nano Lett.*, 2006, **6**, 1529.
110. H. Bonnemann and R. M. Richards, *Eur. J. Inorg. Chem.*, 2001, 2455.
111. Y. Xuan and Q. Li, *Int. J. Heat Fluid Flow*, 2000, **21**, 58.
112. K. Kwak and C. Kim, *Korean-Aust. Rheol. J.*, 2005, **17**, 35.
113. P. Keblinski, J. A. Eastman and D. G. Cahill, *Mater. Today*, 2005, **8**, 36.
114. M. S. Liu, M. C. C. Lin, I. T. Huang and C. C. Wang, *Int. Commun. Heat Mass Transfer*, 2005, **32**, 1202.
115. X. B. Wang, Z. M. Liu, P. A. Hu, Y. Q. Liu, B. X. Han and D. B. Zhu, *Appl. Phys. A: Mater. Sci. Process.*, 2005, **80**, 637.
116. D. Bom, R. Andrews, D. Jacques, J. Anthony, B. Chen, M. S. Meie and J. P. Selegue, *Nano Lett.*, 2002, **2**, 615.
117. S. Suresh, K. P. Venkitaraj, P. Selvakumar and M. Chandrasekar, *Colloids Surf., A*, 2011, **388**, 41.

118. M. M. Ghosh, S. Ghosh and S. K. Pabi, *Nanosci. Nanotechnol. Lett.*, 2012, **4**, 1.
119. Y. Hwang, J. K. Lee, J. K. Lee, Y. M. Jeong, S. Cheong, Y. C. Ahn and S. H. Kim, *Powder Technol.*, 2008, **186**, 145.
120. M. Moosavi, E. K. Goharshadi and A. Youssefi, *Int. J. Heat Fluid Flow*, 2010, **31**, 599.
121. C. Choi, H. S. Yoo and J. M. Oh, *Curr. Appl. Phys.*, 2007, **8**, 710.
122. D. Wen and Y. Ding, *IEEE Trans. Nanotech.*, 2006, **5**, 220.
123. J. M. Salehi, M. M. Heyhat and A. Rajabpour, *Appl. Phys. Lett.*, 2013, **102**, 231907.
124. Y. Li, J. e. Zhou, S. Tung, E. Schneider and S. Xi, *Powder Technol.*, 2009, **196**, 89.
125. Y. Chen, D. L. Peng, D. Lin and X. Luo, *Nanotechnology*, 2007, **18**, 505703.
126. J. Zhu, D. Li, H. Chen, X. Yang, L. Lu and X. Wang, *Mater. Lett.*, 2004, **58**, 3324.
127. S. U. Sandhya and S. A. Nityananda, *Nanomater. Nanotechnol.*, 2013, **3**, 1.
128. S. A. Kumar, K. S. Meenakshi, B. R. V. Narashimhan, S. Srikanth and G. Arthanareeswaranc, *Mater. Chem. Phys.*, 2009, **113**, 57.
129. K. Patel, S. Kapoor, D. P. Dave and T. Mukherjee, *J. Chem. Sci.*, 2005, **117**, 53.
130. H. Akoh, Y. Tsukasaki, S. Yatsuya and A. Tasaki, *J. Cryst. Growth*, 1978, **45**, 495.
131. V. Sridhara and L. N. Satapathy, *Nanoscale Res. Lett.*, 2011, **6**, 1.
132. S. U. S. Choi and J. A. Eastman, *US Pat.*, 6221275B1, 2001.
133. A. G. Kanaras, F. S. Kamounah, K. Schaumburg, C. J. Kiely and M. Brust, *Chem. Commun.*, 2002, **20**, 2294.
134. M. S. Liu, M. C. C. Lin, C. Y. Tsai and C. C. Wang, *Int. J. Heat Mass Transfer*, 2006, **49**, 3028.
135. U. S. Shenoy and A. N. Shetty, *Appl. Nanosci.*, 2014, **4**, 47.
136. M.-S. Liu, M. C.-C. Lin, C. Y. Tsai and C.-C. Wang, *Int. J. Heat Mass Transfer*, 2006, **49**, 3028.
137. F. Xun, Y. Wei, L. Yusheng, W. Debao, S. Huaqiang and Y. Fengyuan, *J. Dispers. Sci. Technol.*, 2005, **26**, 575.
138. Z. Said, M. A. Abdelkareem, H. Rezk, M. A. Nassef and H. Z. Atwany, *Powder Technol.*, 2020, **364**, 795.
139. D. Cabaleiro, P. Estellé, H. Navas, A. Desforges and B. Vigolo, *J. Nanofluids*, 2018, **7**, 1081.
140. C. C. D. Santosa, W. R. Viali, E. D. S. N. Vialib Jr and M. Jafelicci Jr., *J. Mol. Liq.*, 2020, **113**, 113391.
141. C. H. Lo, T. T. Tsung and L. C. Chen, *J. Cryst. Growth*, 2005, **277**, 636.
142. C. H. Lo, T. T. Tsung and H. M. Lin, *J. Alloys Compd.*, 2007, **434–435**, 659.
143. H. J. Kim, I. C. Bang and J. Onoe, *Opt. Lasers Eng.*, 2009, **47**, 532.

144. S. W. Lee, S. D. Park and I. C. Bang, *Int. J. Heat Mass Transfer*, 2012, **55**, 6908.
145. T. X. Phuoc, Y. Soong and M. K. Chyu, *Opt. Lasers in Eng.*, 2007, **45**, 1099.
146. A. R. Sadrolhosseini, S. A. Rashid, A. Zakaria and K. Shameli, *J. Nanomater.*, 2016, **2016**, 1.
147. P. X. Tran and S. Yee, In *ASME Applied Mechanics and Materails Conference*, 2007.
148. V. Piriyawong, V. Thongpool, P. Asanithi and P. Limsuwan, *J. Nanomater.*, 2012, **2012**, 1.
149. M. C. Mbambo, S. Khamlich, T. Khamliche, M. K. Moodley, K. Kaviyarasu, I. G. Madiba, M. J. Madito, M. Khenfouch, J. Kennedy, M. Henini, E. Manikandan and M. Maaza, *Sci. Rep.*, 2020, **10**, 1.
150. P. V. Kazakevich, A. V. Simakin, V. V. Voronov and G. A. Shafeev, *Appl. Surf. Sci.*, 2006, **252**, 4373.
151. A. Riahi, S. Khamlich, M. Balghouthi, T. Khamliche, T. B. Doyle, W. Dimassi, A. Guizani and M. Maaza, *J. Mol. Liq.*, 2020, **304**, 112694.
152. W. K. Woo, Y. M. Hung and X. Wang, *Case Stud. Therm. Eng.*, 2021, **25**, 100993.
153. M. Rafique, M. S. Rafique, U. Kalsoom, A. Afzal, S. H. Butt and A. Usman, *Opt. Quantum Electron.*, 2019, **51**, 1.
154. J. Taha-Tijerina, S. Shaji, S. S. Kanakkillam, M. I. M. Palma and K. Aviña, *Appl. Sci.*, 2020, **10**, 1779.
155. H. Wang, J. Z. Xu, J. J. Zhu and H. Y. Chen, *J. Cryst. Growth*, 2002, **244**, 88.
156. H. T. Zhu, Y. S. Lin and Y. S. Yin, *J. Colloid Interface Sci.*, 2004, **277**, 100.
157. H. Bönnemann, S. S. Botha, B. Bladergroen and V. M. Linkov, *Appl. Organomet. Chem.*, 2005, **19**, 768.
158. A. K. Singh and V. S. Raykar, *Colloid Polym. Sci.*, 2008, **286**, 1667.
159. F. Seifikar and S. Azizian, *Energy Convers. Manage.*, 2021, **228**, 113675.
160. A. V. Nikam and A. H. Dadwal, *Adv. Powder Technol.*, 2019, **30**, 13.
161. F. Bonet, K. Tekaia-Elhsissen and K. V. Sarathy, *Bull. Mater. Sci.*, 2000, **23**, 165.
162. Y. Sun, B. Mayers, T. Herricks and Y. Xia, *Nano Lett.*, 2003, **3**, 955.
163. Y. L. Hsin, K. C. Hwang, F. R. Chen and J. J. Kai, *Adv. Mat.*, 2001, **13**, 830.
164. S. Zeroual, P. Estellé, D. Cabaleiro, B. Vigolo, M. Emo, W. Halim and S. Ouaskit, *J. Mol. Liq.*, 2020, **310**, 113229.
165. L. R. d. Oliveira, S. R. F. L. Ribeiro, M. H. M. Reis, V. L. Cardoso and E. P. B. Filho, *Diam. Relat. Mater.*, 2019, **96**, 216.
166. C. Wanga, J. Yanga and Y. Ding, *Prog. Nat. Sci.*, 2013, **23**, 338.
167. J. Yang, E. Sargent, S. Kelley and J. Y. Ying, *Nat. Mat.*, 2010, **8**, 683.
168. A. Kumar, H. M. Joshi, A. B. Mandale, R. Srivastava, S. D. Adyanthaya, R. Pasricha and M. Sastry, *J. Chem. Sci.*, 2004, **116**, 293.
169. X. Wang, S. Xu, J. Zhou and W. Xu, *J. Colloid Interf. Sci.*, 2010, **348**, 24.
170. W. Yu, H. Xie, X. Wang and X. Wang, *Nanoscale Res. Lett.*, 2011, **6**, 1.

171. H. Zhu, C. Zhang, Y. Tang, J. Wang, B. Ren and Y. Yin, *Carbon*, 2007, **45**, 226.
172. T. Muthukumaran, G. Gnanaprakash and J. Philip, *J. Nanofluids*, 2012, **1**, 85.
173. M. M. Can, S. Ozcan, A. Ceylan and T. Firat, *Mater. Sci. Eng., C*, 2010, **172**, 72.
174. M. Inkyo, Y. Tokunaga, T. Tahara, T. Iwaki, F. Iskandar, C. J. Hogan and K. Okuyama, *Ind. Eng. Chem.*, 2008, **47**, 2597.
175. S. Harjanto, H. Sutanto, R. Setiaji, A. H. Yuwono and D. Ferdian, *AIP Conf. Proc.*, 2011, **1415**, 110.
176. M. J. Nine, B. Munkhbayar, M. S. Rahman, H. Chung and H. Jeong, *Mater. Chem. Phys.*, 2013, **141**, 636.
177. L. Almásy, D. Creanga, C. Nadejde, L. Rosta, E. Pomjakushina and M. Ursache-Oprisan, *J. Serbian Chem. Soc.*, 2014, **80**, 367.
178. S. Tanimoto, Y. Nakamura, H. Yamaoka and Y. Hirokawa, *Int. J. Poly. Sci.*, 2010, 294790.
179. W. g. Kim, H. U. Kang, K.-m. Jung and S. H. Kim, *Sep. Sci. Technol.*, 2008, **43**, 3036.
180. S. M. Abdel-Samad, A. A. Fahmy, A. A. Massoud and A. M. Elbedwehy, *Curr. Nanosci.*, 2017, **13**, 586.
181. D. Jing, Y. Hu, M. Liu, J. Wei and L. Guo, *Sol. Energy*, 2015, **112**, 30.
182. V. M. Goud, V. Vaisakh, M. Joseph and V. Sajith, *Appl. Therm. Eng.*, 2019, **168**, 114862.
183. Z. H. Han, F. Y. Cao and B. Yang, *Appl. Phys. Lett.*, 2008, **92**, 243104.
184. G. Kim, A. Sousa, D. Meyers and M. Libera, *Microsc. Microanal.*, 2008, **14**, 459.
185. M. Joseph and V. Sajith, *Appl. Therm. Eng.*, 2019, **147**, 756.
186. E. V. Jitheesh, M. Joseph and V. Sajith, *Int. Commun. Heat Mass Transfer*, 2021, **127**, 105541.
187. B. A. Bhanvase, S. D. Sayankar, A. Kapre, P. Fule and S. H. Sonawane, *Appl. Therm. Eng.*, 2018, **128**, 134.
188. D. Yao, T. Li, Y. Zheng and Z. Zhang, *React. Funct. Polym.*, 2019, **136**, 131.
189. M. Sarafraz and F. Hormozi, *Exp. Therm. Fluid Sci.*, 2015, **66**, 279.
190. R. Kumar, J. N. Sharma and J. Sood, *Mater. Today: Proc.*, 2020, **28**, 1781.
191. M. S. Jameel, A. A. Aziz and M. A. Dheyab, *Nano-Struct. Nano-Objects*, 2020, **23**, 100484.
192. A. Rufus, N. Sreeju, V. Vilas and D. Philip, *J. Mol. Liq.*, 2017, **242**, 537.
193. G. B. Jegadeesan, K. Srimathi, N. S. Srinivas, S. Manishkanna and D. Vignesh, *Biocatal. Agric. Biotechnol.*, 2019, **21**, 101354.
194. R. Ranjbarzadeh, A. Moradikazerouni, R. Bakhtiari, A. Asadi and M. Afrand, *J. Clean. Prod.*, 2019, **206**, 1089.
195. E. C. Okonkwo, E. A. Essien, E. Akhayere, M. Abid, D. Kavaz and T. A. H. Ratlamwala, *Sol. Energy*, 2018, **170**, 658.
196. S. Omiddezyani, S. Gharehkhani, V. Yousefi-Asli, I. Khazaee, M. Ashjaee, R. Nayebi, F. Shemirani and E. Houshfard, *Colloids Surf., A*, 2021, **610**, 125923.

197. B. T. Sone, A. Diallo, X. G. Fuku, A. Gurib-Fakim and M. Maaza, *Arab. J. Chem.*, 2020, **13**, 160.
198. G. Sharmila, C. Muthukumaran, E. Sangeetha, H. Saraswathi, S. Soundarya and N. M. Kumar, *Nano-Struct. Nano-Objects*, 2019, **20**, 100380.
199. J. L. Luna-Sánchez, J. L. Jiménez-Pérez, R. Carbajal-Valdez, G. Lopez-Gamboa, M. Pérez-González and Z. N. Correa-Pacheco, *Thermochim. Acta*, 2019, **678**, 178314.
200. R. Sadri, M. Hosseini, S. N. Kazi, S. Bagheri, S. M. Ahmed, G. Ahmadi, N. Zubir, M. Sayuti and M. Dahari, *Energy Convers. Manage.*, 2017, **150**, 26.
201. R. Sadri, M. Hosseini, S. N. Kazi, S. Bagheri, N. Zubir, K. H. Solangi, T. Zaharinie and A. Badarudin, *J. Colloid Interface Sci.*, 2017, **504**, 115.
202. S. F. S. Shirazi, S. Gharehkhani, H. Yarmand, A. Badarudin, H. S. C. Metselaar and S. N. Kazi, *Mater. Lett.*, 2015, **152**, 192.
203. N. Pauzi, N. M. Nurul and A. A. Yusof, *J. Environ. Chem. Eng.*, 2020, **8**, 103331.
204. M. Hosseini, H. A. Abdelrazek, R. Sadri, A. R. Mallah, S. N. Kazi, B. T. Chew, S. Rozali and N. Yusoff, *Int. J. Heat Mass Transfer*, 2018, **127**, 403.
205. H. R. Kulkarni, C. Dhanasekaran, P. Rathnakumar and S. Sivaganesan, *Mater. Today: Proc.*, 2021, **42**, 1037.
206. Y. Mostafa Yusefi, S. Kamyar, S. Y. Ong, T. Sin-Yeang, H. Ziba, J. Hossein, W. Thomas J and K. Kuca, *Int. J. Nanomedicine*, 2020, **16**, 2515.
207. S. N. M. Zainon and W. H. Azmi, *Int. Commun. Heat Mass Transfer*, 2021, **126**, 105402.
208. M. M. Sarafraz, A. Arya, V. Nikkhah and F. Hormozi, *Chem. Biochem. Eng. Q.*, 2016, **30**, 489.
209. E. K. Goharshadi, S. Samiee and P. Nancarrow, *J. Colloid Interface Sci.*, 2011, **356**, 473.
210. M. K. Alam, K. Shah, E. Doroodchi, R. Azizian and B. Moghtaderi, *Int. J. Heat Mass Transfer*, 2016, **98**, 778.
211. S. A. Angayarkanni and J. Philip, *J. Phys. Chem. C*, 2013, **117**, 9009.
212. X. Zhang, H. Gu and M. Fujii, *Exp. Therm. Fluid Sci.*, 2007, **31**, 593.
213. M. Bloemen, W. Brullot, T. T. Luong, N. Geukens, A. Gils and T. Verbiest, *J. Nanopart. Res.*, 2012, **14**, 1.
214. S. Gyergyek, D. Makovec and M. Drofenik, *J. Colloid Interface Sci.*, 2011, **354**, 498.
215. Q. Lan, C. Liu, F. Yang, S. Liu, J. Xu and D. Sun, *J. Colloid Interface Sci.*, 2007, **310**, 260.
216. X.-M. Liu and L.-S. Wang, *Biomaterials*, 2004, **25**, 1929.
217. C. Y. Wang, J. M. Hong, G. Chen, Y. Zhang and N. Gu, *Chin. Chem. Lett.*, 2010, **21**, 179.
218. K. Yang, H. Peng, Y. Wen and N. Li, *Appl. Surf. Sci.*, 2010, **256**, 3093.
219. J. Wang, G. Li, T. Li and M. Zeng, *J. Therm. Anal. Calorim.*, 2020, **143**, 4057.

220. I. W. Almanassra, A. D. Manasrah, U. A. Al-Mubaiyedh, T. Al-Ansari, Z. O. Malaibari and M. A. Atieh, *J. Mol. Liq.*, 2020, **304**, 111025.
221. T. J. Choi, S. P. Jang and M. A. Kedzierski, *Int. J. Heat Mass Transfer*, 2018, **122**, 483.
222. L. Vekas, D. BICA and O. Marinica, *Rom. Rep. Phys.*, 2006, **58**, 257.
223. P. K. Das, A. K. Mallik, R. Ganguly and A. K. Santra, *J. Mol. Liq.*, 2018, **254**, 98.
224. S. A. Angayarkanni and J. Philip, *J. Appl. Phys.*, 2015, **118**, 094306.
225. B. Ruan and A. M. Jacobi, *Nanoscale Res. Lett.*, 2012, **7**, 127.
226. I. M. Mahbubul, R. Saidur, M. A. Amalina and M. E. Niza, *Int. Commun. Heat Mass Transfer*, 2016, **76**, 33.
227. P. Garg, J. L. Alvarado, C. Marsh, A. T. Carlson, A. D. Kessler and K. Annamalai, *Int. J. Heat Mass Transfer*, 2009, **52**, 5090.
228. K. Kwak and C. Kim, *Korea Aust. Rheol. J.*, 2005, **17**, 35.
229. H. Akoh, Y. Tsukasaki, S. Yatsuya and A. Tasaki, *J. Cryst. Growth*, 1978, **45**, 495.
230. K. Nemade and S. Waghuley, *Appl. Therm. Eng.*, 2016, **95**, 271.
231. E.-O.-L. Ettefaghi, H. Ahmadi, A. Rashidi, S. S. Mohtasebi and M. Alaei, *Int. J. Ind. Chem.*, 2013, **4**, 28.
232. M. Farbod, R. K. Asl and A. R. N. Abadi, *Colloids Surf., A*, 2015, **474**, 71.
233. B. D. Cullity and S. R. Stock, *Elements of X-Ray Diffraction*, Prentice Hall, London, 2001.
234. B. J. Berne and R. Pecora, *Dynamic light scattering: with applications to biology, chemistry and physics*, John Wiley, New York, 1976.
235. D. B. Williams and C. B. Carter, *Transmission electron microscopy: a textbook for materials science*, Springer, 1996.
236. F. Owens and C. P. Poole Jr., *The physics and chemistry of nanosolids*, John Wiley & Sons, New Jersy, 2008.
237. J. N. Israelachvili, *Intermolecular and surface forces*, Academic Press, San Diego, 1985.
238. V. Gupta and P. Trivedi, in *Lipid Nanocarriers for Drug Targeting*, William Andrew Applied Science, 2018, p. 563.
239. R. J. Hunter, *Zeta potential in colloid science: Principles and applications*, Academic Press, London, 1981.